Low oxygen enhances trophoblast column growth by potentiating the extravillous lineage and promoting LOX activity

Jenna Treissman[1,2], Victor Yuan[1,3], Jennet Baltayeva[1,2], Hoa T. Le[1,2], Barbara Castellana[1,2], Wendy P. Robinson[1,3], Alexander G. Beristain[1,2]

[1] The British Columbia Children's Hospital Research Institute, Vancouver, Canada.
[2] Department of Obstetrics & Gynecology, The University of British Columbia, Vancouver, Canada.
[3] Department of Medical Genetics, The University of British Columbia, Vancouver, Canada.

To whom correspondence should be addressed: Alexander G. Beristain, The British Columbia Children's Hospital Research Institute, The University of British Columbia, Vancouver, British Columbia, Canada. V5Z 4H4. Tel: (604) 875-3573; E-mail: aberista@mail.ubc.ca

Keywords: Hypoxia, placentation, trophoblast, extravillous trophoblast, villous cytotrophoblast, lysyl oxidase

Summary Statement: Low oxygen promotes extravillous trophoblast differentiation

Abbreviations

BAPN:β-aminopropionitrile
BrdU: Bromodeoxyuridine
CM: Conditioned media
CTB: Cytotrophoblast
DAP: 1,5-diaminopentane
DCT: Distal column trophoblast
DGE: Differential gene expression
ECM: Extracellular matrix
EVT: Extravillous trophoblast
FDR: False discovery rate
GO: Gene ontology
HIF1A: Hypoxia inducible factor 1 A
HLA-G: Human leukocyte antigen G
Hr: Hour
IF: Immunofluorescence
LOX: Lysyl oxidase
PCA: Principal component analysis
PCT: Proximal column trophoblast
PEG10: Paternally expressed gene 10
scRNA-seq: single cell RNA sequencing
SCT: Syncytiotrophoblast
UMAP: Uniform manifold approximation and projection
vCTB: Villous cytotrophoblast

ABSTRACT

Early placental development and the establishment of the invasive trophoblast lineage take place within a low oxygen environment. However, conflicting and inconsistent findings have obscured the role of oxygen in regulating invasive trophoblast differentiation. In this study, the effect of hypoxic, normoxic, and atmospheric oxygen on invasive extravillous pathway progression was examined using a human placental explant model. Here, we show that exposure to low oxygen enhances extravillous column outgrowth and promotes the expression of genes that align with extravillous trophoblast (EVT) lineage commitment. By contrast, super-physiological atmospheric levels of oxygen promote trophoblast proliferation while simultaneously stalling EVT progression. Low oxygen-induced EVT differentiation coincided with elevated transcriptomic levels of lysyl oxidase (*LOX*) in trophoblast anchoring columns, where functional experiments established a role for LOX activity in promoting EVT column outgrowth. The findings of this work support a role for low oxygen in potentiating the differentiation of trophoblasts along the extravillous pathway. Additionally, these findings generate insight into new molecular processes controlled by oxygen during early placental development.

INTRODUCTION

In mammalian development, the placenta forms the mechanical and physiological link between maternal and fetal circulations. In rodents and humans that have invasive haemochorial placentae, nutrient and oxygen transfer between mother and fetus is achieved through extensive uterine infiltration by placenta-derived cells of epithelial lineage called trophoblasts (Pijnenborg et al., 2011; Velicky et al., 2016). In humans, trophoblast differentiation into invasive cell subtypes, called extravillous trophoblast (EVT), is essential for optimal placental function (Tilburgs et al., 2015; Velicky et al., 2016). Molecular processes governing invasive EVT differentiation and specific EVT functions like uterine artery remodeling and immuno-modulation of maternal leukocytes are strictly controlled (Pollheimer et al., 2018; Wallace et al., 2012). Defects in trophoblast differentiation along the EVT pathway associate with impaired placental function and certain aberrant conditions of pregnancy that directly impact fetal and maternal health (Avagliano et al., 2012).

In early pregnancy, anchoring villi of the placental basal plate initiate cellular differentiation events leading to the formation of EVT. At specific villi-uterine attachment points, proliferative EVT progenitors establish multi-layered cellular structures called anchoring columns (Haider et al., 2016; Pollheimer et al., 2018). Trophoblasts residing within proximal regions of anchoring columns, termed proximal column trophoblasts (PCT), are highly proliferative and show evidence of initial molecular characteristics that are hallmarks of EVT (Haider et al., 2018; Turco et al., 2018). At distal regions within anchoring columns, column trophoblasts lose their proliferative phenotype and express many markers akin to invasive EVT, such as HLA-G, α5 and β1 integrins, NOTCH2, and ERBB2 (Fock et al., 2015a; Fock et al., 2015b; Haider et al., 2016; Kabir-Salmani et al., 2004; Zhou et al., 1997). The transition of PCT into distal column trophoblasts (DCT) represents a significant developmental step towards the formation of uterine-invading and tissue-remodeling EVT.

Anchoring columns of the placenta initially develop in the absence of maternal blood, and

subsequently, within a relatively low oxygen environment (~20 mmHg) (Jauniaux et al., 2000; Jauniaux et al., 1999; Rodesch et al., 1992). By comparison, the partial pressure of arterial blood oxygen is approximately 100 mmHg, while the partial pressure of oxygen within the placental bed by 14 weeks' gestation is estimated to be between 40-60 mmHg (Jauniaux et al., 2001). The role of oxygen in controlling anchoring column formation and EVT differentiation has been the focus of many studies (Caniggia et al., 2000; Genbacev et al., 1997; James et al., 2006; Lash et al., 2006; Wakeland et al., 2017). Unfortunately, contradictory and inconsistent findings have obscured the role of oxygen tension in controlling aspects of trophoblast biology, where low oxygen both promotes (Caniggia et al., 2000; Genbacev et al., 1997) and restrains (James et al., 2006; Lash et al., 2006) column outgrowth, and potentiates (Wakeland et al., 2017) and inhibits (Caniggia et al., 2000; Genbacev et al., 1997) EVT differentiation. These reported differences on the effect of oxygen on anchoring column outgrowth and EVT differentiation are likely attributed to differences in model platforms and methods used to isolate, characterize, and culture trophoblasts. Nonetheless, the role of oxygen in controlling anchoring column formation and column trophoblast differentiation has yet to be fully examined.

In this study, we examine how differing levels of oxygen affect first trimester placental column outgrowth. Using placental villous tissue explants that recapitulate many of the morphological and molecular events central to anchoring column formation and EVT differentiation *in vivo*, we show that low levels of oxygen potentiate column outgrowth. We demonstrate that low oxygen drives hypoxia-related gene programs and processes central to cell-extracellular matrix interaction, while exposure to high oxygen promotes/maintains a strong proliferative phenotype. Moreover, we provide evidence that supports a role for low levels of oxygen in promoting the differentiation of column trophoblasts along the EVT pathway. We further identify *LOX* as a critical gene up-regulated in response to low oxygen that supports column outgrowth, and provide important insight into novel molecular programs impacted by oxygen that align with trophoblast differentiation along the EVT pathway.

114 **RESULTS**

115 **Hypoxia potentiates trophoblast column outgrowth**

116 To test the effect of exposure to differing levels of oxygen on trophoblast column establishment
117 and outgrowth, we utilized a Matrigel-imbedded placental explant model that closely reproduces
118 developmental processes of trophoblast column cell expansion and differentiation along the EVT
119 pathway (Bilban et al., 2009; Newby et al., 2005). Early column formation during human placental
120 development is characterized by the expansion of mitotically active $Ki67^{+}$/HLA-G^{lo} proximal column
121 trophoblasts (PCT) into HLA-G^{hi} non-proliferating distal column trophoblasts (DCT) and invasive
122 EVT (Figure 1A, 1B). To this end, Matrigel-imbedded placental explants recapitulate anchoring
123 column cell organization and EVT-lineage commitment, establishing the explant system as an
124 appropriate experimental tool to study the cellular and molecular underpinnings regulating human
125 trophoblast column formation and outgrowth (Figure 1C).

126 Chorionic villi harvested from early first trimester placentae (n=8; 5-8 weeks' gestation) were
127 imbedded into Matrigel matrix and allowed to establish for 24 hr at 5% oxygen (Figure 2A); this level
128 of oxygen represents a relative "normoxic" condition for early placental development (Jauniaux et al.,
129 2001). Characteristics (age, gestational age, BMI, smoking status) of each patient who donated their
130 placenta for explant culture are listed in Supplemental Table 1. Following this, explants derived from
131 the same placenta were transferred into one of three conditions for an additional 48 hr representing
132 either hypoxic (1%, ~10 mmHg O_2), normoxic (5%, ~35 mmHg O_2), or hyperoxic (20%, ~141 mmHg
133 O_2) environments relative to the first trimester of pregnancy (Figure 2A). Within all oxygen conditions,
134 explant outgrowth was observed (Figure 2B, 2C). However, column outgrowth was most pronounced
135 in 1% and 5% oxygen, where outgrowth area in both of these low oxygen conditions was significantly
136 greater than outgrowth observed in 20% oxygen (Figure 2C, 2D). While column outgrowth in 5%
137 oxygen was overall less variable and trended on producing smaller columns than explants cultured in

138 1% oxygen, there was no statistical difference between outgrowth in 1% and 5% oxygen (Figure 2D).
139 In summary, trophoblast column outgrowth was potentiated by low oxygen, whereas exposure to
140 atmospheric oxygen (20% oxygen) blunted column outgrowth.
141
142 **Explant exposure to low or high levels of oxygen generate distinct transcriptomic signatures**
143 To gain mechanistic insight into how hypoxic, physiologically normal, and high levels of
144 oxygen modulate trophoblast column outgrowth, global gene expression was analysed in placental
145 explant cultures using gene microarrays. For this experiment, placental explants from 5 unique
146 placentae (n=5; 5-7 weeks' gestation) were established as previously described except that cultures
147 were maintained in their respective oxygen condition (1%, 5%, or 20%) for 24 hr prior to RNA
148 isolation in order to capture molecular signatures central to column formation. Importantly, RNA was
149 extracted from only column trophoblasts and Matrigel-invading EVT; chorionic villi of explants were
150 carefully micro-dissected away from columns and EVT following an approach described within Bilban
151 *et al* (Bilban et al., 2009) (Figure 3A). Following standard probe filtering, and normalization
152 (Supplemental Figure 1), differential gene expression (DGE) analysis of explant trophoblasts was
153 performed. Using a false discover rate (FDR) < 0.05, we identified many differences in gene
154 expression between 1% versus 20% (293 genes up-regulated; 685 genes down-regulated) and 5%
155 versus 20% oxygen conditions (363 genes up-regulated; 406 genes down-regulated) (Figure 3B;
156 Supplemental Table 2). DGE analysis between 1% and 5% oxygen did not identify differentially
157 expressed genes (Figure 3B). Principal component analysis (PCA) shows clustering of explants
158 cultured in hypoxic, normoxic, and hyperoxic conditions (Figure 3C). PCA sample clustering showed
159 explant trophoblasts cultured in 1% and 5% oxygen generally clustered closer together, save for two
160 1% oxygen explant outliers; one clustered amongst 20% oxygen samples while the other clustered
161 separately to all other samples (Figure 3C). Despite these two explants being identified as significant

162 outliers using the Silhouette coefficient (Barghash and Arslan, 2016), we opted to retain them for the
163 remainder of our analyses as we could not confidently ascribe outlier classification due to technical or
164 batch-related artifacts.

165 Hierarchical clustering of the 15 column trophoblast samples segregated samples into two
166 statistically significant clusters (*sigclust*, $p<0.05$): a 20% oxygen dominated cluster and a cluster
167 comprised of column trophoblasts cultured in 1% and 5% oxygen (Figure 3D). A gene heat-map of the
168 top 40 differentially expressed genes (top 20 differentially expressed genes in 1%; top 20 differentially
169 expressed genes in 20%; FDR< 0.05, ranked by FC) highlights gene patterns across 1%, 5%, and 20%
170 oxygen cultures (Figure 3D). In both 1% and 5% oxygen conditions, the top hits identified by global
171 DGE analysis included genes associated with hypoxia (*EGLN3, RORA*), cell-matrix interaction/re-
172 structuring (*LOX, JAM2, EGLN3, PLAUR*), and gene transcription regulation (*MXI1, TSC22D3,*
173 *RORA*). In contrast, the most highly expressed genes in explants exposed to 20% oxygen were
174 exclusive to pro-mitotic/proliferative processes (*MKI67, KIF20A, KIF23, PEG10, CDK1, NCAPG,*
175 *NCAPH, TOP2A, CDC7*), indicating that column trophoblasts cultured in 20% oxygen possess a
176 proliferative phenotype.

177 While stringent DGE parameters did not identify differentially expressed genes between 1%
178 and 5% oxygen culture conditions, we did identify 123 and 53 unique genes to be up-regulated in 5%
179 and 1% oxygen cultures compared to samples cultured in 20% oxygen (Figure 3E). Further, 78 and 357
180 genes were shown to be uniquely down-regulated in 5% and 1% oxygen cultured explants compared to
181 20% cultures (Figure 3F). Gene ontology (GO) pathway analysis of the above 1% and 5% signatures
182 indicated that column trophoblasts exposed to 1% oxygen show enrichment for processes favoring
183 hypoxia-related- and oxidative stress-signaling (Supplemental Figure 2). Conversely, column
184 trophoblasts cultured in 5% oxygen showed enrichment of biological pathways linked to nucleotide
185 biosynthesis and metabolism, indicating that column trophoblasts in 1% and 5% oxygen do exhibit

186 underlying molecular differences potentially contributing to trophoblast column development
187 (Supplemental Figure 2).
188
189 **Differing oxygen levels drive distinct molecular programs in trophoblast columns**
190 To broadly examine how transcriptomic differences within column trophoblasts exposed to
191 hypoxic, normoxic, and hyperoxic conditions relate to differences in molecular pathways, gene
192 signatures determined by DGE analysis (FDR < 0.05; fold-change > 1.5; Supplemental Table 2) were
193 used to identify pathways enriched in explant column trophoblasts cultured in 1%, 5%, and 20%
194 oxygen. Unsurprisingly, pathways in explants cultured in 1% oxygen (293 genes; clusterProfiler)
195 showed enrichment for multiple pathways and molecular processes specific to hypoxia (Figure 4A).
196 Additionally, the 1% oxygen signature also showed enrichment for pathways related to extracellular
197 matrix (ECM) structure and organization, steroid hormone responses, and hydroxyproline metabolism
198 (Figure 4A). Similar to the 1% oxygen pathway readouts, the 5% oxygen signature (363 genes) showed
199 enrichment for genes specific to ECM composition, response to hypoxia, and response to steroid
200 hormones, but also showed enrichment of pathways related to bone development and viral entry into
201 cells (Supplemental Figure 3). By contrast, 20% oxygen (685 genes) showed enrichment of pathways
202 and cellular processes related to organelle fission, nuclear division, chromosome segregation, mitotic
203 nuclear division, and DNA packaging and replication, all of which link to heightened cell cycle activity
204 and proliferation (Figure 4B).
205 Using the Mitotic Nuclear Division, Chromosome Segregation, and DNA Replication curated
206 GO gene signatures enriched within 20% column trophoblasts (93 genes; Supplemental Table 3),
207 explant samples were subjected to hierarchical clustering and visualized by gene heat-map (Figure 4C).
208 Notably, samples segregated into two groups: One group defined by 1% oxygen samples (4/5 1%
209 oxygen samples), and the other group consisting of mostly of 5% and 20% oxygen samples (10/10

210 5%/20% samples) (Figure 4C). This later branch was further divided into two sub-branches, one
211 enriched by 5% oxygen samples also containing a 1% oxygen sample outlier, and the other sub-branch
212 made up entirely of 20% oxygen column trophoblasts (Figure 4C). Interestingly, gene heat-map
213 expression intensities suggest a step-wise increase in expression of pro-mitotic/proliferative genes in
214 column trophoblasts exposed to increasing levels of oxygen (Figure 4C). To verify if an increase in
215 exposure to oxygen tension translates into increased proliferation, a BrdU pulse-chase was performed
216 on a separate cohort of placental explants (n=3) cultured in 1%, 5%, and 20% oxygen. In support of the
217 gene array data, little/no evidence of cell proliferation within explant columns was observed in 1%
218 oxygen cultures following a 4 hr chase (Figure 4D, 4E). However, explants cultured in 5% oxygen
219 showed a significant increase in BrdU incorporation within column trophoblasts compared to 1%
220 oxygen columns, and an even greater level of BrdU positivity was measured within 20% oxygen
221 columns (20% versus 1%) (Figure 4D, 4E). Though a trend for greater proliferation in explant columns
222 cultured in 20% oxygen compared to 5% oxygen was observed, this difference was not significant
223 (Figure 4E). Overall, our findings suggest that explant column trophoblasts cultured in low oxygen up-
224 regulate molecular processes related to hypoxia/HIF1A signalling and ECM organization/remodeling,
225 while column trophoblasts exposed to hyper-physiological 20% oxygen adopt a predominantly pro-
226 proliferative phenotype.
227
228 **Low oxygen promotes EVT differentiation**
229 Differentiation of trophoblasts along the EVT pathway is in part defined by the exiting of PCT
230 located at the base of anchoring columns from the cell cycle (Velicky et al., 2018). Moreover, as
231 column trophoblasts located at distal portions of columns acquire pro-invasive EVT-like
232 characteristics, molecular pathways related to ECM-remodeling and protease functions are accordingly
233 up-regulated (Davies et al., 2016). Our observation that low oxygen (1% & 5%) promotes

234 transcriptional signatures linked to cell-ECM interaction and protease-ECM remodeling, while 20%
235 oxygen promotes proliferation, suggests that exposure to low oxygen drives, while high oxygen
236 restrains EVT differentiation.

237 To gain insight into how differing levels of oxygen affect column trophoblast differentiation,
238 explant column trophoblasts were subjected to hierarchical cluster analysis using a signature of
239 differentially expressed genes derived from a list of 47 trophoblast-related genes curated from recent
240 high-dimensional data and differentiation studies focused on trophoblast biology (Supplemental Figure
241 4; Supplemental Table 4) (Bilban et al., 2009; Davies et al., 2016; Haider et al., 2018; Lee et al., 2018;
242 Turco et al., 2018). This list includes genes associated with trophoblast lineage (*TFAP2A, KLF5,*
243 *GATA3*), trophoblast pluripotency (*CDX2*), villous cytotrophoblast (CTB) state (*EGFR, SPINT1,*
244 *ITGA6, PEG10, TEAD4, TP63*), EVT state (*HLA-G, HTRA1, LAIR2, FLT-1, ERBB2, ADAM12,*
245 *AMAM19, MYC, ITGA5, TEAD2*), syncytiotrophoblast (SCT) state (*GCM1, CGA, ERVW1, ERVFRD-1,*
246 *ENDOU*), and genes commonly used to identify proliferative CTB and PCT (*MK167, CCNA2,*
247 *NOTCH1*). From this curated list, 14 genes were differentially expressed between 1%, 5%, and 20%
248 oxygen cultured explants (Supplemental Figure 4A). Notably, this small signature was sufficient to
249 segregate samples into two main groups: One group consisted almost entirely of column trophoblasts
250 cultured in 20% oxygen (save for one 1% oxygen outlier), while the other group was made up of a mix
251 of 1% and 5% oxygen cultured samples (Supplemental Figure 4A). Genes enriched within low-oxygen
252 cultured explants included trophoblast lineage-related transcription factors (*GATA3*, *KLF5*, *TFAP2A*),
253 genes related to ECM remodeling (*TIMP1*, *ADAM12, ADAM19*), genes related to CTB specification
254 (*CDH1*, *EGFR*), and genes linked with the EVT sub-lineage (*ADAM12*, *FLT1*, *ITGA5, MYC*)
255 (Supplemental Figure 4A). Samples that grouped primarily as 20% oxygen cultured explants showed
256 enrichment for genes specific to proliferative CTB and PCT (*CCNA2*, *MKI67*). Notably, the imprinted
257 paternally expressed gene, *PEG10*, was also highly expressed within 20% oxygen column trophoblasts

258 (Supplemental Figure 4A).

259 Examination of PEG10 localization within first trimester placental villi (n=3 placentae; 6-10
260 weeks' gestation) by immunofluorescence microscopy (IF) showed that PEG10 preferentially localizes
261 to CTB (Supplemental Figure 4B). IF localization of PEG10 within a new cohort of placental explants
262 (established from n=5 placentae) revealed that PEG10 signal, similar to the signal observed in placental
263 villi, is broadly localized to CTB in explants exposed to all three oxygen culture conditions
264 (Supplemental Figure 4C). However, within 20% oxygen explants, bright PEG10 signal was also
265 observed within multi-layered PCT; this column-specific signal was minimal/absent in 1% and 5%
266 oxygen cultures (Supplemental Figure 4C).

267 To more closely examine how global gene expression changes identified within low and high
268 oxygen exposed explants relate to trophoblast differentiation, we examined the expression of the top
269 fifteen up-regulated genes in column trophoblasts cultured in 1% and 20% oxygen (FDR < 0.05; fold-
270 change > 2) within a recently reported first trimester placenta single cell transcriptomic dataset (Vento-
271 Tormo et al., 2018). Using this dataset we focused exclusively on the 5 subtypes of trophoblasts that
272 were described (14,366 trophoblasts from 5 individual placentae): CTB, proliferative CTB, SCT,
273 proliferative EVT (likely PCT), and EVT (likely an admixture of DCT and invasive EVT) (Figure 5A)
274 (Vento-Tormo et al., 2018). Within UMAP-directed cell clusters, the specificity of each trophoblast
275 sub-lineage/type is shown by expression levels of *EGFR* (CTB), *ERVFRD-1* (syncytin-2; SCT), *HLA-G*
276 (column trophoblast & EVT), and *MKI67* (proliferating trophoblast) (Figure 5B). A heat-map
277 projection shows the pattern of gene expression of trophoblast lineage and subtype-specific genes (Pan
278 trophoblast: *KRT7, TFAP2A, GATA3, KLF5*; CTB: *EGFR, SPINT1, TP63*; proliferative CTB and PCT:
279 *MKI67, CCNA2*; SCT: *ENDOU, ERVFRD-1*; EVT: *HLA-G, ITGA5, ERBB2*), and the fifteen top up-
280 regulated genes in 20% (*OAS1, IFIT3, DLGAP5, GSTA3, CDK1, OXCT1, CENPF, KIF20A, PARP1,*
281 *TOP2A, PLEKHH1, RFX5, NCPAH, KPNA2, NRP2*) and 1% oxygen conditions (*TNFSF10, LOX,*

282 *AKAP12, ACTC1, BIRC7, SPNS2, S100A4, JAM2, MXI1, EGLN3, RORA, PLAUR, AK4, TSC22D3,*
283 *NRN1*) (Figure 5C). Interestingly, genes up-regulated within 1% oxygen-cultured columns showed
284 alignment with proliferative EVT, and this relationship was even greater with EVT (Figure 5C). In
285 contrast, the top genes identified within 20% oxygen columns aligned predominately with proliferative
286 CTB and proliferative EVT (Figure 5C).

287 Pseudotime trajectory analysis using a gene signature derived from the top 1000 variable genes
288 reproduced a lineage trajectory similar to that reported in Vento-Tormo *et al* (Vento-Tormo et al.,
289 2018), where a predicted cell origin state was identified as well as the two differentiation trajectories
290 aligning with the villous and extravillous pathways (Figure 5D). Correlating the expression of genes
291 specific to distinct states of trophoblast differentiation (i.e. *EGFR, HLA-G, ERVFRD-1*) with the
292 pseudotime trajectory confirmed the accuracy of the pseudotime modeling, where *EGFR* aligned to
293 cells committed to the villous pathway, *HLA-G* to a maturing EVT, and *ERVFRD-1* to a terminally
294 differentiated SCT (Figure 5E). Correlating trophoblast lineage trajectory with the top up-regulated 1%
295 and 20% oxygen genes showed that genes enriched within 20% oxygen aligned to both the villous and
296 extravillous pathway trajectories (Figure 5F). Notably, high-oxygen genes aligned closely with cell
297 states linked to proliferative CTB (*PARP1, RFX5, PLEKHH1, GSTA3, NRP2*) and proliferative PCT
298 (*OXCT1, KIF20A, NCAPH, CENPF, TOP2A, DLGAP5, CDK1, KPNA2*) (Figure 5F). By contrast, low
299 oxygen enriched genes primarily aligned with the tail-end of the extravillous pathway (i.e. *TNFSF10,*
300 *LOX, SPNS2, S100A4, JAM2, PLAUR*) (Figure 5F). Together, these data suggest that column
301 trophoblasts exposed to low oxygen adopt transcriptomic signatures that are reflective of EVT, while
302 column trophoblasts cultured in 20% oxygen express genes that align predominately with proliferating
303 CTB and PCT.
304
305

306 ***LOX* expression and activity is potentiated by low oxygen**

307 Our finding that low oxygen drives column outgrowth and potentiates the expression of genes
308 linked with the EVT phenotype suggests that genes highly expressed within low oxygen columns may
309 in part contribute to EVT differentiation and trophoblast column formation. Rank ordering of up-
310 regulated genes by fold-change in both 1% and 5% oxygen column trophoblasts identified multiple
311 conserved genes between the two oxygen conditions (Supplemental Table 2). Notably, *LOX*, the gene
312 encoding lysyl oxidase, a copper-dependent enzyme that catalyses collagen and elastin crosslinking,
313 was the number 2-ranked gene in both 1% and 5% oxygen cultured explants. Specifically, *LOX*
314 expression was 6.2- and 5.1-fold higher in 1% and 5% oxygen cultures compared to 20% oxygen
315 explants (Figure 6A; Supplemental Table 2). While previous work has identified a role for elevated
316 *LOX* expression in promoting tumor cell metastasis (Cox et al., 2015; Di Stefano et al., 2016), the role
317 of LOX in placental trophoblast column biology and trophoblast differentiation along the EVT pathway
318 has not been described.

319 As an initial step to examine the importance of LOX in anchoring column biology, *LOX* mRNA
320 *in situ* hybridization within first trimester placental villi (n=3; 6-8 weeks' gestation) was performed.
321 RNAscope *in situ* hybridization showed specific and intense *LOX* localization to cells within the
322 mesenchymal core of placental villi and to trophoblasts within anchoring columns (Figure 6B).
323 Little/no *LOX* signal was detected in CTB or SCT (Figure 6B). RNAscope analysis of *LOX* within
324 placental explants cultured in 1% and 20% oxygen supported the gene array finding that *LOX*
325 expression was elevated in column trophoblasts exposed to low oxygen (Figure 6C). While we were
326 unable to verify elevated LOX protein expression in low oxygen-cultured placental explants via IF
327 microscopy due to non-specific antibody signal, LOX enzymatic activity, measured in conditioned
328 media (CM) generated by placental explants cultured in 1% or 20% oxygen, showed that activity was
329 significantly higher in 1% cultures (Figure 6D). Use of the LOX inhibitor, β-aminopropionitrile

330 (BAPN), demonstrated LOX-substrate specificity, while recombinant active LOX served as a positive
331 control (Figure 6D). Taken together, these findings show that LOX expression and activity is elevated
332 in column trophoblasts cultured in low oxygen. Further, *LOX's* preferential *in vivo* expression within
333 the trophoblast anchoring column combined with its involvement in promoting tumor cell metastasis,
334 suggests that LOX may also play a role in controlling trophoblast column outgrowth and/or EVT
335 differentiation.
336
337 **Impairment of LOX restrains column outgrowth**
338 To test the function of LOX in column outgrowth, Matrigel-imbedded placental explants
339 cultured in 1% oxygen (n=3) were cultured in either control explant media or media containing the
340 competitive LOX inhibitor BAPN. The effectiveness of BAPN in inhibiting LOX activity was
341 measured as before by examining the ability of endogenous LOX in explant CM to oxidize substrate
342 (Figure 7A). Conditioned media harvested from control explants showed LOX activity levels slightly
343 below levels measured in recombinant LOX positive control reactions, but significantly higher than
344 explant media alone (Figure 7A). Importantly, treatment of explants with BAPN significantly blunted
345 LOX activity, though activity was not completely blocked (Figure 7A). Importantly, placental explant
346 treatment with BAPN led to a significant two-fold impairment in column outgrowth (Figure 7B, 7C).
347 Taken together, these results suggest that LOX expression in developing trophoblast columns promotes
348 column outgrowth and associates with an EVT phenotype.
349

350 **DISCUSSION**

351 Here we describe how exposure to different levels of oxygen differentially affect trophoblast
352 column outgrowth and global gene expression. We provide evidence that exposure to low oxygen
353 results in overall increases in column outgrowth accompanied by gene expression signatures that align
354 with an EVT phenotype. By contrast, gene signatures in high oxygen-cultured column trophoblasts
355 define a role for elevated oxygen in maintaining column growth through cell proliferation. In both
356 hypoxic and normoxic conditions, we identify the gene *LOX*, as one of the most highly up-regulated
357 genes within explant columns. We show that *LOX* expression associates with EVT lineage trajectory
358 and demonstrate that impairment of LOX activity blunts column outgrowth. Together, this work
359 supports a role for low oxygen in potentiating the EVT pathway. Moreover, this work also identifies
360 novel oxygen-sensitive molecular processes that likely play roles in anchoring column formation
361 during human placental development.

362 The role of oxygen in controlling column formation and the EVT pathway is controversial.
363 Previous studies have shown that exposure of placental explants to low oxygen (i.e. 2% to 3% oxygen)
364 promotes column expansion and outgrowth, where outgrowth is primarily attributed to HIF1A-directed
365 cell proliferation (Caniggia et al., 2000; Genbacev et al., 1997). Consistent with this, evidence exists
366 that CTB exposure to low oxygen restrains trophoblast progression along the EVT pathway (Caniggia
367 et al., 2000; Genbacev et al., 1997; Lash et al., 2006). By contrast, rodents and rodent-derived
368 trophoblast stem cells engineered to lack hypoxia-sensing machinery (i.e. *ARNT*, *HIF1A,* and/or *EPSA1*
369 null) fail to differentiate into trophoblast lineages of the labyrinth zone and into trophoblast giant cells,
370 trophoblast populations akin to invasive EVT in humans (Chakraborty et al., 2016; Chakraborty et al.,
371 2011; Cowden Dahl et al., 2005; Gultice et al., 2009; Maltepe et al., 2005). In support of these
372 observations, low oxygen was shown to potentiate an invasive phenotype in human primary
373 trophoblasts with an accompaniment in the expression of EVT-associated genes HLA-G and α5

374 integrin, and the up-regulation of pro-migratory integrin-linked kinase signaling (Horii et al., 2016;
375 Robins et al., 2007; Wakeland et al., 2017). Our findings overall align with these later studies that
376 suggest low oxygen promotes differentiation along the EVT pathway. Notably, we show that low
377 oxygen drives expression of EVT-related genes and signatures that align with EVT lineage trajectory.
378 We show that low oxygen (1% and 5% oxygen) induces expression of hallmark EVT genes like
379 *ITGA5*, *ADAM12*, and *FLT1*, as well as the transcription factors *KLF5* and *GATA3* that are
380 preferentially expressed by EVT. Importantly, the use of cell lineage trajectory modeling using single
381 cell RNA sequencing data also provides evidence that low oxygen promotes a cell state consistent with
382 the EVT lineage. These later observations are in line with the association of low levels of oxygen
383 within the intervillous space and anchoring column formation and interstitial EVT infiltration into
384 decidual mucosa in early pregnancy. However, the relationship between relative placental hypoxia and
385 inadequate placentation in aberrant pregnancy conditions like preeclampsia (Farrell et al., 2019)
386 suggests that the impact of oxygen on trophoblast biology may differ according to stage of
387 development.

388 Our finding that high levels of oxygen promote column trophoblast proliferation is inconsistent
389 with previous studies investigating the role of hypoxia in anchoring column biology (Caniggia et al.,
390 2000; Genbacev et al., 1997). However, in agreement with our findings, James *et al* reported that
391 explant columns cultured in 8% oxygen have increased trophoblast cellularity compared with columns
392 exposed to 1.5% oxygen (James et al., 2006). Moreover, there seems to be consistent agreement that
393 exposure to low oxygen leads to greater column outgrowth, where oxygen tension levels between 1-5%
394 consistently generate larger columns than atmospheric oxygen conditions (Caniggia et al., 2000; James
395 et al., 2006). However, dissecting how enhanced column outgrowth is achieved, i.e. via greater cell
396 proliferation within the column or through increased trophoblast migration and invasion, is still not
397 completely resolved. Indeed, while our data suggests that low oxygen promotes an EVT phenotype and

398 enhances molecular pathways related to cell-ECM remodeling, we did not directly examine if low
399 oxygen affects EVT invasion. The stark differences on the effect of oxygen levels in regulating
400 trophoblast proliferation and EVT differentiation within explant columns between various studies is
401 difficult to explain, but may stem from differences in media composition, the matrix substratum used in
402 explant cultures, subtle variations in oxygen tension, and the gestational age of placental tissues/cells
403 used for establishing explant cultures. Future studies will need to specifically re-examine how differing
404 levels of oxygen impact column cell proliferation.

405 *PEG10*, a paternally expressed and maternally imprinted gene, was identified as a top up-
406 regulated gene within 20% oxygen column trophoblasts. Previous work has shown a critical role for
407 Peg10 in mouse placental development, where mice deficient in Peg10 show severe fetal growth
408 restriction and fetal demise by E10.5, in addition to defects in labyrinth and spongiotrophoblast
409 development (Ono et al., 2006). Intriguingly, a partial loss in *Peg10* imprinting leading to *Peg10* over-
410 expression also associates with impaired labyrinth formation (Koppes et al., 2015). These findings
411 suggest that a fine balance in Peg10 expression is required for proper placental development. Notably,
412 in humans, dysregulation of PEG10 associates with certain pregnancy disorders, including pre-
413 eclampsia, gestational hypertension, molar pregnancy, and spontaneous miscarriage (Dória et al., 2010;
414 Liang et al., 2014; Rahat et al., 2017). Our finding that *PEG10* expression and cell proliferation in
415 trophoblast columns associates with exposure to high oxygen is consistent with studies showing a role
416 for PEG10 in promoting tumor cell survival and growth (Bang et al., 2015; Ishii et al., 2017; Peng et
417 al., 2017). Recent findings also provide evidence that PEG10 promotes trophoblast cell line
418 proliferation (Abed et al., 2019). Given that PEG10 specifically localizes to CTB of floating villi and to
419 subsets of trophoblasts within proximal regions of anchoring columns suggests that PEG10 may play
420 roles in column establishment by promoting progenitor expansion. Further work is needed to dissect
421 the role of PEG10 in column formation and progression along the EVT pathway.

422 Our finding that *LOX* expression was consistently a gene highly up-regulated in both 1% and
423 5% column trophoblasts compared to those cultured in 20% oxygen indicates that LOX-related
424 processes are important in placental development and trophoblast column biology. While a role of
425 LOX in column formation has not been previously reported, the importance of LOX in tumorigenesis is
426 known, where elevated LOX associates with numerous types of cancers and LOX activity promotes
427 tumor cell metastasis (Cox et al., 2015; Di Stefano et al., 2016). Further, a recent report does provide
428 evidence that LOX expression promotes cell invasion of a trophoblast cell line (Xu et al., 2019). This
429 later finding is consistent with the association of LOX expression and the EVT phenotype. Aldehydes
430 produced by LOX-directed oxidation of lysine residues within collagen and elastin facilitate
431 collagen/elastin cross-linking and stability, which in turn provide a structural lattice for cell movement
432 (Kim et al., 2014). That *LOX* expression is greatest within both proximal and distal column
433 trophoblasts is interesting, as PCT are not considered to be migratory. Nonetheless, it is likely that
434 creating an appropriate substratum scaffold via LOX-directed collagen crosslinking may contribute to
435 column stability and provide a platform for EVT outgrowth. How or if LOX affects anchoring column
436 establishment or EVT differentiation is unknown, but future studies utilizing newly-derived trophoblast
437 organoids (Haider et al., 2018; Turco et al., 2018) may allow for deep mechanistic examination of LOX
438 and the EVT pathway.
439 In summary, the extravillous pathway is controlled by multiple intrinsic as well as extrinsic
440 factors, including level of oxygen. We provide evidence that supports a role for low oxygen levels in
441 promoting the differentiation of trophoblasts along the EVT pathway. This finding establishes insight
442 into critical developmental events during placentation that occur in early pregnancy. Further, these
443 findings may also provide a foundation for understanding cellular and molecular processes contributing
444 to conditions linked to aberrant placentation.
445

446 **MATERIALS AND METHODS**

447 **Patient recruitment and tissue collection**

448 Decidual and placental tissues were obtained with approval from the Research Ethics Board on the use
449 of human subjects, University of British Columbia (H13-00640). All samples were collected from
450 women (19 to 39 years of age) providing written informed consent undergoing elective terminations of
451 pregnancy at British Columbia's Women's Hospital, Vancouver, Canada. First trimester decidual
452 (*N*=1) and placental tissues (*N*=30) were collected from participating women (gestational ages ranging
453 from 5–12 weeks) having confirmed viable pregnancies by ultrasound-measured fetal heartbeat. The
454 decidual tissue sample was selected based on the presence of a smooth uterine epithelial layer and a
455 textured thick spongy underlayer. Patient clinical characteristics i.e. height and weight were
456 additionally obtained to calculate body mass index (BMI: kg/m^2) and all consenting women provided
457 self-reported information via questionnaire to having first hand exposure to cigarette smoke, and are
458 summarized in Supplemental Table 1.

459

460 **Placental villous explant assay**

461 *Ex vivo* placental villous cultures were established as described in (Aghababaei et al., 2014; De
462 Luca et al., 2017; Perdu et al., 2016). Briefly, placental villi from 5-8 week old gestation placentas
463 (n=8) obtained from patients undergoing elective termination of pregnancy were dissected, washed in
464 cold PBS, and imbedded into Millicell cell culture inserts (0.4 μm pores, 12mm diameter. EMD
465 Millipore, Billerica, MA) containing 200 μl of growth-factor-reduced Phenol-red free Matrigel (BD
466 Biosciences, San Diego, CA). Explants, containing 400 μl DMEM/F12 1:1 (200 mM L-glutamine) in
467 the outer chamber, were allowed to establish overnight in a humidified 37 °C trigas incubator at 5%
468 oxygen, 5% CO_2. Following 24 hr of culture, explants were cultured in 200 μl DMEM/F12 1:1 media
469 and placed into 1%, 5%, or 20% oxygen incubators for either an additional 24 hr (gene expression

470 analyses) or 48 hr (explant outgrowth measurements). All explant media were supplemented with
471 penicillin/streptomycin and antimycotic solution (Thermofisher Scientific, Waltham, MA) Growing
472 explants were imaged at indicated times using a Nikon SMZ 7454T triocular dissecting microscope
473 (Minato, Japan) outfitted with a digital camera. EVT outgrowths were measured by ImageJ software.
474 Fold-change in outgrowth was determined by dividing the mean column area at 48 hr into the mean
475 area at 0 hr.
476
477 **Immunofluorescence, RNAScope, and immunohistochemistry microscopy**
478 *Immunofluorescence:* Placental villi (6-12 weeks gestation; n=5) or placental explants (derived
479 from n=11 placentae) were fixed in 2% paraformaldehyde overnight at 4 °C. Tissues were paraffin
480 embedded and sectioned at 6 μm onto glass slides. Immunofluorescence was performed as described
481 elsewhere (Aghababaei et al., 2015). Briefly, cells or placental tissues underwent antigen retrieval by
482 heating slides in a microwave for 5 X 2 minute intervals in a citrate buffer (pH 6.0). Sections were
483 incubated with sodium borohydride for 5 minutes, RT, followed by Triton X-100 permeabilization for
484 5 minutes, RT. Slides were blocked in 5% normal goat serum/0.1% saponin for 1h, RT, and incubated
485 with combinations of the indicated antibodies overnight, 4 °C: Anti-HLA-G (1:100, 4H84, Exbio,
486 Vestec, Czech Republic); anti-cytokeratin 7, mouse monoclonal IgG (1:50, RCK105, Santa Cruz
487 Biotechnology, Dallas, TX); anti-cytokeratin 7, rabbit monoclonal IgG (1:50, SP52, Ventana Medical
488 Systems, Oro Valley, AZ); anti-Ki67 (1:75, SP6, Thermo Fisher Scientific); anti-LOX (1:100, NB100-
489 2527, NovusBio, Centennial, CO); anti-PEG10 (1:100, 4C10A7, NovusBio); anti-BrdU (1:1000,
490 Bu20a, Cell Signalling Technology, Danvers, MA). Following overnight incubation, sections and
491 coverslips were washed with PBS and incubated with Alexa Fluor goat anti rabbit-488/-568 and goat
492 anti mouse-488/-568 conjugated secondary antibodies (Life Technologies, Carlsbad, CA) for 1 hr at RT
493 and washed in PBS, and mounted using ProLong Gold mounting media containing DAPI (Life

494 Technologies).

495 Slides were imaged with an AxioObserver inverted microscope (Car Zeiss, Jena, Germany)
496 using 20X Plan-Apochromat/0.80NA or 40X Plan-Apochromat oil/1.4NA objectives (Carl Zeiss). An
497 ApoTome .2 structured illumination device (Carl Zeiss) set at full Z-stack mode and 5 phase images
498 was used for image acquisition. For quantification of BrdU signal in column trophoblasts, 2-4 cell
499 columns per explant (n=9; obtained using a 20X objective) were used to calculate values; BrdU+ cell
500 proportions were calculated by BrdU/KRT7+ cells per column; BrdU fluorescence intensity thresholds
501 were used to calculate BrdU proportions within Matrigel explant columns. Images were obtained using
502 an Axiocam 506 monochrome digital camera and processed and analyzed using ZenPro software (Carl
503 Zeiss).

504 *Immunohistochemistry:* Decidua (10 weeks' gestation; n=1) from a first trimester pregnancy
505 was fixed in 2% paraformaldehyde for 24 hr at 4°C, paraffin imbedded, and serially sectioned at 6µm
506 onto glass slides. Heat-induced antigen retrieval was performed using sodium citrate (10mM, pH 6.0)
507 followed by quenching endogenous peroxidases with 3% hydrogen peroxide for 30 minutes at RT.
508 Sections were then permeabilized with 0.2% Triton-X-100 for 5 minutes at RT. Serum block was
509 performed with 5% BSA in tris-buffered saline with 0.05% Tween 20 (TBST). Sections were then
510 incubated with mouse monoclonal HLA-G (1:100, clone 4H84, ExBio) diluted in TBST overnight at
511 4°C. Following overnight incubation, sections were incubated with Envision+ Dual Link Mouse/Rabbit
512 HRP-linked secondary antibody (DAKO, Santa Clara, CA) for 1 hr at RT. IgG1 isotype controls and
513 secondary antibody-only negative controls were performed to confirm antibody specificity. Staining
514 was developed via 3,3'-diaminobenzidine (DAB) chromogen (DAB Substrate Kit, Thermo Scientific),
515 counterstained in Modified Harris Hematoxylin Solution (Sigma-Aldrich, St. Louis, MO) and
516 coverslips mounted with Entellan mounting medium (Electron Microscopy Sciences, Hatfield, PA).

517 *RNAScope:* RNA *in situ* hybridization was performed using RNAscope® 2.5 HD Assay-RED

518 (Advanced Cell Diagnostics, Newark, CA) following the manufacturer's instructions (Wang *et al.*,
519 2012). Briefly, placenta (n = 3; 6-8 weeks' gestation) and Matrigel-imbedded placental explants (n=15;
520 5 explants per oxygen condition) from first trimester pregnancies were fixed overnight at 4°C in 4%
521 paraformaldehyde and paraffin-embedded. Tissue sections were serially sectioned at 6 µm, and
522 following deparaffinization, antigen retrieval was performed using RNAscope® Target Retrieval
523 Reagent (95°C for 15 minutes) and ACD Protease Plus Reagent (40°C for 30 minutes). RNAScope
524 probes targeting LOX (Hs-LOX-C2; Ref. 415941-C2) and negative control (Probe-dapB; Ref. 310043)
525 were incubated on sections for 2hr at 40°C, and following this, the RNAscope signal was amplified
526 over 6 rounds of ACD AMP 1-6 incubation and application of RED-A and RED-B at a ratio of 1
527 volume of RED-B to 60 volumes of RED-A for 10 minutes at RT. Selected samples were
528 counterstained with 50% Hematoxylin I for 2 minutes at RT and all samples were mounted using
529 EcoMount (Biocare Medical, Pacheco, CA).
530
531 **RNA purification**
532 Total RNA was prepared from column and invasive EVT cells using TRIzol reagent (Life
533 Technologies, Carlsbad, CA) followed by RNeasy MinElute Cleanup (Qiagen, Hilden, Germany) and
534 DNase treatment (Life Technologies) according to the manufacturer's instructions. Care was taken so
535 that explants were exposed to atmospheric oxygen no longer than 2 minutes during microscopic
536 dissection and separation of placental villi away from columns prior to the addition of TRIzol. RNA
537 purity was confirmed using a NanoDrop Spectrophotometer (Thermo Fisher Scientific) and by running
538 RNA samples on an Agilent 2100 Bioanalyzer (Agilent Technologies, Santa Clara, CA). Only RNA
539 samples having an RNA Integrity Number (RIN) > 8.0 were used.
540
541

542 **Microarray hybridization, gene array data preprocessing, gene expression analysis**

543 Total RNA samples extracted from explant columns were sent to Génome Québec Innovation
544 Centre (McGill University, Montréal, Canada) for RNA quantification. Briefly, RNA samples were
545 prepared for transcriptome profiling using the GeneChip ™ Pico Reagent Kit (Thermo Fisher
546 Scientific) as per manufacturer's protocol. Samples were run on the Clariom™ S Human Array to
547 measure gene expression at >20,000 genes in the human genome (Affymetrix, Santa Clara, CA). Raw
548 data generated from the arrays were read into R statistical software (version 3.5.1) with the
549 Bioconductor *oligo* package to convert raw Affymetrix CEL files into an expression matrix of intensity
550 values. The expression data was background corrected, Quantile normalized, and log-transformed. A
551 total of 13,787 control, duplicated, non-annotated or low intensity probes were filtered out of the data,
552 leaving 13,402 probes for further analysis. Pre-processing was monitored at each step by Principal
553 Component Analysis (PCA) and linear modelling. Principal component analysis was performed by the
554 `svd()` function from the *`sva`* package in R. Linear modelling was conducted using the R package
555 *limma*. Probe-wise variances were shrunk using empirical Bayes with the `eBayes` function, followed
556 by FDR adjustment for multiple testing (Benjamini and Hochberg, 1995). Differentially expressed
557 genes were defined based on an FDR < 0.05. Enrichment of pathways were identified and annotated
558 using the *clusterProfiler* package in Bioconductor (Carvalho and Irizarry, 2010). Volcano plots were
559 generate using the *ggplot2* package for RStudio. Cluster analysis of sample relations based on principal
560 components was generated using the `plotSampleRelation` function for the *Lumi* package. A
561 hierarchical cluster analysis was conducted using Euclidean distances on the top 40 differentially
562 expressed genes, selected by FDR <0.05 and ranked by fold-change > 1.5.

563

564 **Single cell RNA-seq data analysis**

565 Processed droplet-based and Smart-seq2 single cell RNA sequencing data was obtained from public

566 repositories (ArrayExpress experiment codes: E-MTAB-6701 and E-MTAB-6678) (Vento-Tormo et
567 al., 2018). Cells belonging to clusters from trophoblast lineages (n=14,366) were merged from droplet-
568 based and Smart-seq2 data, and corrected for batch-effects using canonical correlation analysis
569 implemented in the R package *Seurat* (Butler et al., 2018). Pseudotime trajectory modelling was
570 conducted using the *monocle 2* R package (Qiu et al., 2017; Trapnell et al., 2014) under the
571 recommended unsupervised procedure called "`dpFeature`". Briefly, the first 10 principal
572 components on log-normalized expression data were used to construct a TSNE projection, upon which
573 density-peak clustering determined 13 number of clusters, using parameters rho = 2, delta = 10. The top
574 1000 differentially expressed genes between these clusters were then used for ordering the cells.
575 Visualization of oxygen concentration -dependent genes were visualized along the inferred
576 pesudotime-ordered branches using the R function
577 `monocle::plot_genes_branched_heatmap` with the following settings: the number of
578 clusters k = 5 for clustering the genes, and default parameters for all else.
579

580 **LOX activity assay and LOX inhibition**

581 Measurement of endogenous LOX activity in placental explant conditioned media was
582 performed following a modified protocol described in Wiel et al (Wiel et al., 2013). Briefly, 600 μl of
583 conditioned media from placental explants cultured in triplicate from either 1%, 5%, or 20% oxygen
584 conditions was pooled, concentrated 12-fold using 7.5 kDa exclusion Amicon Millipore concentration
585 columns (Millipore, Burlington, MA), and snap-frozen in liquid nitrogen. LOX activity in 15 μl of
586 concentrated conditioned media was determined using the Amplex Red H_2O_2 detection kit following
587 the manufacture's instructions (Life Technologies, Carlsbad, CA). This assay is based on the ability of
588 endogenous LOX to oxidize 10 mM DAP (a LOX substrate) in the presence of 0.5 U/ml horseradish
589 peroxidase; the reaction is incubated at 37 °C for 30 minutes. Oxidation of Amplex Red generates a

590 fluorescence signal measurable at 560nm/590nm excitation/emission wavelengths and was detected
591 using a fluorescence plate reader (BMG Labtech, Ortenberg, Germany) using a 96-well format. As a
592 positive control, 10 μg/ml recombinant active LOX (MyBioscource.com, San Diego, CA) was
593 separately incubated with DAP substrate. LOX activity/specificity was determined by co-incubating
594 reactions with 5 mM of BAPN. For endogenous inhibition of LOX within explant cultures, following
595 24 hr of explant establishment at 37 °C, 5% CO2, 5% O2 in a humidified tri-gas incubator, explant
596 media was replaced with media containing 500 μM of BAPN and explant cultures were placed into 1%
597 or 20% O_2 culture conditions for an additional 48 hr of culture prior to being imaged/measured.
598
599 **BrdU incorporation assay**
600 Pulse-chase labeling with BrdU (Sigma-Aldrich) was conducted on a verification cohort of
601 Matrigel embedded placental explants (n=3 distinct placentae, 4-11 columns per oxygen condition).
602 Explants were established in 5% oxygen for 24 hr followed by 24 hr of culture in either 1%, 5% or
603 20% oxygen. After 48 hr of culture, explants were exposed to a 4-hr pulse with culture media
604 containing 10μM of BrdU. Following 4 hr of labelling, explants were washed in PBS and fixed in 4%
605 PFA overnight. Explants were paraffin embedded and sectioned for immunofluorescence microscopy.
606 Immunofluorescent staining with anti-BrdU antibody (Bu20a, Sigma-Aldrich) with the addition of a
607 30-minute incubation in 2M hydrochloric acid between permeabilization and sodium borohydride
608 steps.
609
610 **Statistical analysis**
611 Data are reported as median values with standard deviations. All calculations were carried out
612 using GraphPad Prism software (San Diego, CA). For single comparisons, Mann-Whitney non-
613 parametric unpaired t-tests were performed. For multiple comparisons, one-way Kruskal-Wallis

614 ANOVA followed by Dunn's multiple comparison test was performed on explant outgrowth data as
615 outgrowth in 1% oxygen was not normally distributed. One-way ANOVA followed by Tukey post-test
616 were performed for all other multiple comparisons. The differences were accepted as significant at $P <$
617 0.05. For gene microarray and scRNA-seq statistical analyses, please refer to the Gene Array Data
618 Preprocessing and scRNA-seq analysis sections in methods.
619
620

621 **DATA AVAILABILITY/ACCESSION NUMBER**

622 The GEO accession number for the data reported in this paper is: GSE132421

623

624 **AUTHOR CONTRIBUTIONS**

625 AGB designed the research. AGB, JT, VY, JB, HL, and BC performed experiments and
626 analysed data. AGB, JT, VY, and WPR wrote the paper. All authors read and approved the manuscript.

627

628 **FUNDING**

629 This work was supported by a Natural Sciences and Engineering Research Council of Canada
630 (NSERC; RGPIN-2014-04466) Discovery Grant (to AGB), Canadian Institutes of Health Research
631 (CIHR; 201403MOP-325905; 201809PJT-407571-CIA-CAAA) operating grants to AGB, and a CIHR
632 Master's graduate studentship (to JT).

633

634 **ACKNOWLEDGEMENTS**

635 The authors extend their sincere gratitude to the hard work of staff at British Columbia's
636 Women's Hospital's CARE Program for recruiting participants to our study, and thank Dr. Megan K.
637 Barker, for her critical readings of the manuscript.

638

639 **COMPETING INTERESTS**

640 The authors declare that no competing interests exist.

641

642 **REFERENCES**
643

644 **Abed, M., Verschueren, E., Budayeva, H., Liu, P., Kirkpatrick, D. S., Reja, R., Kummerfeld, S.**
645 **K., Webster, J. D., Gierke, S., Reichelt, M., et al.** (2019). The Gag protein PEG10 binds to RNA
646 and regulates trophoblast stem cell lineage specification. *PLoS ONE* **14**, e0214110.

647 **Aghababaei, M., Hogg, K., Perdu, S., Robinson, W. P. and Beristain, A. G.** (2015). ADAM12-
648 directed ectodomain shedding of E-cadherin potentiates trophoblast fusion. *Cell Death Differ.* **22**,
649 1970–1984.

650 **Aghababaei, M., Perdu, S., Irvine, K. and Beristain, A. G.** (2014). A disintegrin and
651 metalloproteinase 12 (ADAM12) localizes to invasive trophoblast, promotes cell invasion and
652 directs column outgrowth in early placental development. *Mol. Hum. Reprod.* **20**, 235–249.

653 **Avagliano, L., Marconi, A. M., Romagnoli, S. and Bulfamante, G. P.** (2012). Abnormal spiral
654 arteries modification in stillbirths: the role of maternal prepregnancy body mass index. **25**, 2789–
655 2792.

656 **Bang, H., Ha, S. Y., Hwang, S. H. and Park, C.-K.** (2015). Expression of PEG10 Is Associated with
657 Poor Survival and Tumor Recurrence in Hepatocellular Carcinoma. *Cancer Res Treat* **47**, 844–852.

658 **Becht, E., McInnes, L., Healy, J., Dutertre, C.-A., Kwok, I. W. H., Ng, L. G., Ginhoux, F. and**
659 **Newell, E. W.** (2018). Dimensionality reduction for visualizing single-cell data using UMAP. *Nat.*
660 *Biotechnol.* **37**, 38–44.

661 **Benjamini, Y. and Hochberg, Y.** (1995). Controlling the False Discovery Rate: A Practical and
662 Powerful Approach to Multiple Testing. *Journal of the Royal Statistical Society: Series B*
663 *(Methodological)* **57**, 289–300.

664 **Bilban, M., Haslinger, P., Prast, J., Klinglmüller, F., Woelfel, T., Haider, S., Sachs, A., Otterbein,**
665 **L. E., Desoye, G., Hiden, U., et al.** (2009). Identification of novel trophoblast invasion-related
666 genes: heme oxygenase-1 controls motility via peroxisome proliferator-activated receptor gamma.
667 *Endocrinology* **150**, 1000–1013.

668 **Butler, A., Hoffman, P., Smibert, P., Papalexi, E. and Satija, R.** (2018). Integrating single-cell
669 transcriptomic data across different conditions, technologies, and species. *Nat. Biotechnol.* **36**,
670 411–420.

671 **Caniggia, I., Mostachfi, H., Winter, J., Gassmann, M., Lye, S. J., Kuliszewski, M. and Post, M.**
672 (2000). Hypoxia-inducible factor-1 mediates the biological effects of oxygen on human trophoblast
673 differentiation through TGFbeta(3). *J. Clin. Invest.* **105**, 577–587.

674 **Carvalho, B. S. and Irizarry, R. A.** (2010). A framework for oligonucleotide microarray
675 preprocessing. *Bioinformatics* **26**, 2363–2367.

676 **Chakraborty, D., Cui, W., Rosario, G. X., Scott, R. L., Dhakal, P., Renaud, S. J., Tachibana, M.,**
677 **Rumi, M. A. K., Mason, C. W., Krieg, A. J., et al.** (2016). HIF-KDM3A-MMP12 regulatory
678 circuit ensures trophoblast plasticity and placental adaptations to hypoxia. *Proc. Natl. Acad. Sci.*
679 *U.S.A.* **113**, E7212–E7221.

680 **Chakraborty, D., Rumi, M. A. K., Konno, T. and Soares, M. J.** (2011). Natural killer cells direct
681 hemochorial placentation by regulating hypoxia-inducible factor dependent trophoblast lineage
682 decisions. *Proc. Natl. Acad. Sci. U.S.A.* **108**, 16295–16300.

683 **Cowden Dahl, K. D., Fryer, B. H., Mack, F. A., Compernolle, V., Maltepe, E., Adelman, D. M.,**
684 **Carmeliet, P. and Simon, M. C.** (2005). Hypoxia-inducible factors 1alpha and 2alpha regulate
685 trophoblast differentiation. *Molecular and Cellular Biology* **25**, 10479–10491.

686 **Davies, J. E., Pollheimer, J., Yong, H. E. J., Kokkinos, M. I., Kalionis, B., Murthi, P., Davies, J.**
687 **E., Yong, H. E. J., Kokkinos, M. I., Kalionis, B., et al.** (2016). Epithelial-mesenchymal transition
688 during extravillous trophoblast differentiation. *Cell Adhesion & Migration* **10**, 310–321.

689 **De Luca, L. C., Le, H. T., Mara, D. L. and Beristain, A. G.** (2017). ADAM28 localizes to HLA-
690 G(+) trophoblasts and promotes column cell outgrowth. *Placenta* **55**, 71–80.

691 **Dória, S., Sousa, M., Fernandes, S., Ramalho, C., Brandão, O., Matias, A., Barros, A. and**
692 **Carvalho, F.** (2010). Gene expression pattern of IGF2, PHLDA2, PEG10 and CDKN1C imprinted
693 genes in spontaneous miscarriages or fetal deaths. *Epigenetics* **5**, 444–450.

694 **Farrell, A., Alahari, S., Ermini, L., Tagliaferro, A., Litvack, M., Post, M. and Caniggia, I.** (2019).
695 Faulty oxygen sensing disrupts angiomotin function in trophoblast cell migration and predisposes
696 to preeclampsia. *JCI Insight* **4**.

697 **Fock, V., Plessl, K., Draxler, P., Otti, G. R., Fiala, C., Knöfler, M. and Pollheimer, J.** (2015a).
698 Neuregulin-1-mediated ErbB2-ErbB3 signalling protects human trophoblasts against apoptosis to
699 preserve differentiation. *J. Cell. Sci.* **128**, 4306–4316.

700 **Fock, V., Plessl, K., Fuchs, R., Dekan, S., Milla, S. K., Haider, S., Fiala, C., Knöfler, M. and**
701 **Pollheimer, J.** (2015b). Trophoblast subtype-specific EGFR/ERBB4 expression correlates with
702 cell cycle progression and hyperplasia in complete hydatidiform moles. *Hum. Reprod.* **30**, 789–
703 799.

704 **Genbacev, O., Zhou, Y., Ludlow, J. W. and Fisher, S. J.** (1997). Regulation of human placental
705 development by oxygen tension. *Science* **277**, 1669–1672.

706 **Gultice, A. D., Kulkarni-Datar, K. and Brown, T. L.** (2009). Hypoxia-inducible factor 1alpha
707 (HIF1A) mediates distinct steps of rat trophoblast differentiation in gradient oxygen. *Biology of*
708 *Reproduction* **80**, 184–193.

709 **Haider, S., Meinhardt, G., Saleh, L., Fiala, C., Pollheimer, J. and Knöfler, M.** (2016). Notch1
710 controls development of the extravillous trophoblast lineage in the human placenta. *Proc. Natl.*
711 *Acad. Sci. U.S.A.* **113**, E7710–E7719.

712 **Haider, S., Meinhardt, G., Saleh, L., Kunihs, V., Gamperl, M., Kaindl, U., Ellinger, A., Burkard,**
713 **T. R., Fiala, C., Pollheimer, J., et al.** (2018). Self-Renewing Trophoblast Organoids Recapitulate
714 the Developmental Program of the Early Human Placenta. *Stem Cell Reports* **11**, 537–551.

715 **Horii, M., Li, Y., Wakeland, A. K., Pizzo, D. P., Nelson, K. K., Sabatini, K., Laurent, L. C., Liu,**
716 **Y. and Parast, M. M.** (2016). Human pluripotent stem cells as a model of trophoblast
717 differentiation in both normal development and disease. *Proc. Natl. Acad. Sci. U.S.A.* **113**, E3882–

718 91.

719 **Ishii, S., Yamashita, K., Harada, H., Ushiku, H., Tanaka, T., Nishizawa, N., Yokoi, K., Washio,**
720 **M., Ema, A., Mieno, H., et al.** (2017). The H19-PEG10/IGF2BP3 axis promotes gastric cancer
721 progression in patients with high lymph node ratios. *Oncotarget* **8**, 74567–74581.

722 **James, J. L., Stone, P. R. and Chamley, L. W.** (2006). The effects of oxygen concentration and
723 gestational age on extravillous trophoblast outgrowth in a human first trimester villous explant
724 model. *Human Reproduction* **21**, 2699–2705.

725 **Jauniaux, E., Watson, A. and Burton, G.** (2001). Evaluation of respiratory gases and acid-base
726 gradients in human fetal fluids and uteroplacental tissue between 7 and 16 weeks' gestation. *YMOB*
727 **184**, 998–1003.

728 **Kabir-Salmani, M., Shiokawa, S., Akimoto, Y., Sakai, K. and Iwashita, M.** (2004). The role of
729 alpha(5)beta(1)-integrin in the IGF-I-induced migration of extravillous trophoblast cells during the
730 process of implantation. *Molecular Human Reproduction* **10**, 91–97.

731 **Koppes, E., Himes, K. P. and Chaillet, J. R.** (2015). Partial Loss of Genomic Imprinting Reveals
732 Important Roles for Kcnq1 and Peg10 Imprinted Domains in Placental Development. *PLoS ONE*
733 **10**, e0135202.

734 **Lash, G. E., Otun, H. A., Innes, B. A., Bulmer, J. N., Searle, R. F. and Robson, S. C.** (2006). Low
735 oxygen concentrations inhibit trophoblast cell invasion from early gestation placental explants via
736 alterations in levels of the urokinase plasminogen activator system. *Biol. Reprod.* **74**, 403–409.

737 **Lee, C. Q. E., Turco, M. Y., Gardner, L., Simons, B. D., Hemberger, M. and Moffett, A.** (2018).
738 Integrin α2 marks a niche of trophoblast progenitor cells in first trimester human placenta.
739 *Development* **145**, dev162305.

740 **Liang, X. Y., Chen, X., Jin, Y. Z., Chen, X. O. and Chen, Q. Z.** (2014). Expression and significance
741 of the imprinted gene PEG10 in placenta of patients with preeclampsia. *Genet. Mol. Res.* **13**,
742 10607–10614.

743 **Maltepe, E., Krampitz, G. W., Okazaki, K. M., Red-Horse, K., Mak, W., Simon, M. C. and**
744 **Fisher, S. J.** (2005). Hypoxia-inducible factor-dependent histone deacetylase activity determines
745 stem cell fate in the placenta. *Development* **132**, 3393–3403.

746 **Newby, D., Marks, L., Cousins, F., Duffie, E. and Lyall, F.** (2005). Villous explant culture:
747 characterization and evaluation of a model to study trophoblast invasion. *Hypertens Pregnancy* **24**,
748 75–91.

749 **Ono, R., Nakamura, K., Inoue, K., Naruse, M., Usami, T., Wakisaka-Saito, N., Hino, T., Suzuki-**
750 **Migishima, R., Ogonuki, N., Miki, H., et al.** (2006). Deletion of Peg10, an imprinted gene
751 acquired from a retrotransposon, causes early embryonic lethality. *Nat. Genet.* **38**, 101–106.

752 **Peng, Y.-P., Zhu, Y., Yin, L.-D., Zhang, J.-J., Wei, J.-S., Liu, X., Liu, X.-C., Gao, W.-T., Jiang,**
753 **K.-R. and Miao, Y.** (2017). PEG10 overexpression induced by E2F-1 promotes cell proliferation,
754 migration, and invasion in pancreatic cancer. *J. Exp. Clin. Cancer Res.* **36**, 30.

755 **Perdu, S., Castellana, B., Yooona, K., Chan, K., DeLuca, L. and Beristain, A. G.** (2016). Maternal
756 obesity drives functional alterations in uterine NK cells. *JCI Insight* **1**.

757 **Pijnenborg, R., Vercruysse, L. and Carter, A. M.** (2011). Deep trophoblast invasion and spiral artery
758 remodelling in the placental bed of the chimpanzee. *Placenta* **32**, 400–408.

759 **Pollheimer, J., Vondra, S., Baltayeva, J., Beristain, A. G. and Knöfler, M.** (2018). Regulation of
760 Placental Extravillous Trophoblasts by the Maternal Uterine Environment. *Front Immunol* **9**, 297.

761 **Qiu, X., Mao, Q., Tang, Y., Wang, L., Chawla, R., Pliner, H. A. and Trapnell, C.** (2017). Reversed
762 graph embedding resolves complex single-cell trajectories. *Nat. Methods* **14**, 979–982.

763 **Rahat, B., Mahajan, A., Bagga, R., Hamid, A. and Kaur, J.** (2017). Epigenetic modifications at
764 DMRs of placental genes are subjected to variations in normal gestation, pathological conditions
765 and folate supplementation. *Sci Rep* **7**, 40774.

766 **Robins, J. C., Heizer, A., Hardiman, A., Hubert, M. and Handwerger, S.** (2007). Oxygen tension
767 directs the differentiation pathway of human cytotrophoblast cells. *Placenta* **28**, 1141–1146.

768 **Tilburgs, T., Crespo, Â. C., van der Zwan, A., Rybalov, B., Raj, T., Stranger, B., Gardner, L.,**
769 **Moffett, A. and Strominger, J. L.** (2015). Human HLA-G+ extravillous trophoblasts: Immune-
770 activating cells that interact with decidual leukocytes. *Proc. Natl. Acad. Sci. U.S.A.* **112**, 7219–
771 7224.

772 **Trapnell, C., Cacchiarelli, D., Grimsby, J., Pokharel, P., Li, S., Morse, M., Lennon, N. J., Livak,**
773 **K. J., Mikkelsen, T. S. and Rinn, J. L.** (2014). The dynamics and regulators of cell fate decisions
774 are revealed by pseudotemporal ordering of single cells. *Nat. Biotechnol.* **32**, 381–386.

775 **Turco, M. Y., Gardner, L., Kay, R. G., Hamilton, R. S., Prater, M., Hollinshead, M. S.,**
776 **McWhinnie, A., Esposito, L., Fernando, R., Skelton, H., et al.** (2018). Trophoblast organoids as
777 a model for maternal-fetal interactions during human placentation. *Nature* **213**, 1.

778 **Velicky, P., Knöfler, M. and Pollheimer, J.** (2016). Function and control of human invasive
779 trophoblast subtypes: Intrinsic vs. maternal control. *Cell Adhesion & Migration* **10**, 154–162.

780 **Velicky, P., Meinhardt, G., Plessl, K., Vondra, S., Weiss, T., Haslinger, P., Lendl, T., Aumayr, K.,**
781 **Mairhofer, M., Zhu, X., et al.** (2018). Genome amplification and cellular senescence are
782 hallmarks of human placenta development. *PLoS Genet.* **14**, e1007698.

783 **Vento-Tormo, R., Efremova, M., Botting, R. A., Turco, M. Y., Vento-Tormo, M., Meyer, K. B.,**
784 **Park, J.-E., Stephenson, E., Polański, K., Goncalves, A., et al.** (2018). Single-cell reconstruction
785 of the early maternal-fetal interface in humans. *Nature* **563**, 347–353.

786 **Wakeland, A. K., Soncin, F., Moretto-Zita, M., Chang, C.-W., Horii, M., Pizzo, D., Nelson, K. K.,**
787 **Laurent, L. C. and Parast, M. M.** (2017). Hypoxia Directs Human Extravillous Trophoblast
788 Differentiation in a Hypoxia-Inducible Factor–Dependent Manner. *The American Journal of*
789 *Pathology* **187**, 767–780.

790 **Wallace, A. E., Fraser, R. and Cartwright, J. E.** (2012). Extravillous trophoblast and decidual
791 natural killer cells: a remodelling partnership. *Hum. Reprod. Update* **18**, 458–471.

792 **Wang, F., Flanagan, J., Su, N., Wang, L.-C., Bui, S., Nielson, A., Wu, X., Vo, H.-T., Ma, X.-J. and**
793 **Luo, Y.** (2012). RNAscope: a novel in situ RNA analysis platform for formalin-fixed, paraffin-
794 embedded tissues. *J Mol Diagn* **14**, 22–29.

795 **Wiel, C., Augert, A., Vincent, D. F., Gitenay, D., Vindrieux, D., Le Calvé, B., Arfi, V., Lallet-**
796 **Daher, H., Reynaud, C., Treilleux, I., et al.** (2013). Lysyl oxidase activity regulates oncogenic
797 stress response and tumorigenesis. *Cell Death Dis* **4**, e855–e855.

798 **Xu, X.-H., Jia, Y., Zhou, X., Xie, D., Huang, X., Jia, L., Zhou, Q., Zheng, Q., Zhou, X., Wang, K.,**
799 **et al.** (2019). Downregulation of lysyl oxidase and lysyl oxidase-like protein 2 suppressed the
800 migration and invasion of trophoblasts by activating the TGF-β/collagen pathway in preeclampsia.
801 *Exp. Mol. Med.* **51**, 20.

802 **Zhou, Y., Fisher, S. J., Janatpour, M., Genbacev, O., Dejana, E., Wheelock, M. and Damsky, C.**
803 **H.** (1997). Human cytotrophoblasts adopt a vascular phenotype as they differentiate. A strategy for
804 successful endovascular invasion? *J. Clin. Invest.* **99**, 2139–2151.

805

806

807 **TITLES AND LEGENDS TO FIGURES**

808 **Figure 1.** Establishment of a human placental villous explant model. **(A)** Schematic illustration
809 showing trophoblast subtypes within placental villus, anchoring column, and maternal uterine tissue.
810 Depicted are villous cytotrophoblasts (CTB), syncytiotrophoblast (SCT), proximal and distal column
811 trophoblast (PCT & DCT), and invasive interstitial and endovascular EVT. **(B)** Immunofluorescence
812 and immunohistochemistry images showing Ki67 (red) and HLA-G (green, brown) expression in
813 human first trimester placental (8 weeks' gestation) and decidual (10 weeks' gestation) tissues. Shown
814 are villous cytotrophoblasts (CTB), proximal and distal column trophoblasts (PCT & DCT), interstitial
815 EVT (iEVT), and the mesenchymal core (MC). Bar = 100 μm. **(C)** Images showing gross villous
816 explant establishment and outgrowth as well as localization of KRT7 (magenta; white), HLA-G
817 (green), and Ki67 (magenta) to specific subtypes of trophoblasts within explant columns. Nuclei are
818 shown via DAPI staining (white). Bar = 100 μm.

819

820 **Figure 2.** Exposure to low oxygen promotes trophoblast column outgrowth. **(A)** Schematic illustration
821 depicting the experimental approach to establishing and culturing placental explants in 1%, 5%, and
822 20% oxygen. **(B)** Representative images showing how explant column outgrowth area is measured at 0
823 hr and 48 hr of culture. The direction of explant outgrowth/invasion is also indicated. **(C)**
824 Representative images of villous explants (n=8 distinct placentae; multiple explants per placenta)
825 cultured in 1%, 5%, and 20% oxygen. Shown within the inverted (invert) image is the area of column
826 outgrowth at 48 hr of culture. **(D)** Bar with scatter plots showing the fold-change of column outgrowth
827 between 48 hr and 0 hr of exposure to 1%, 5%, or 20% oxygen. Median values and standard deviations
828 are shown. Statistical analyses between groups were performed using ANOVA and two-tailed Dunn's
829 post-test; significance considered $p < 0.05$.
830
831

832 **Figure 3.** Comparison of global gene expression patterns between trophoblast columns exposed to 1%,
833 5%, and 20% oxygen. **(A)** Schematic illustration highlighting the removal of placental villi and
834 retention of column trophoblasts and invasive EVT for gene expression analysis. **(B)** Volcano plots
835 showing individual gene-targeting probes differentially expressed between 1% and 20%, 5% and 20%,
836 and 1% and 5% oxygen cultures. X-axis: coefficients from linear model in log2 scale; y axis: negative
837 log base 10 of the false discovery rate (FDR). Black circles indicate probes with an FDR > 0.05; blue
838 and orange circles indicate under-expressed and over-expressed probes with an FDR < 0.05. **(C)** PCA
839 of 1% (blue), 5% (purple), and 20% (red) oxygen cultured explants. **(D)** Dendrogram depicts
840 hierarchical clustering of 1%, 5%, and 20% oxygen cultured column trophoblasts using Z-scores from
841 the top 40 (DEGS from 1% vs 20% comparisons) genes; n=5 per oxygen group. Within the heatmap,
842 brown = low expression; white = mid-level expression; green = high expression. For each sample,
843 oxygen condition (1% = blue; 5% = purple; 20% = red) is indicated, as is the unique placental
844 sample/patient ID used to generate the explant (indicated by shade of grey). Venn diagram showing the
845 number of shared and unique genes (FDR < 0.05) **(E)** up-regulated and **(F)** down-regulated in 1% and
846 5% oxygen-cultured explants compared to 20% oxygen cultures.

847

848

849 **Figure 4.** Placental explant exposure to atmospheric oxygen promotes column trophoblast
850 proliferation. Gene ontology (GO) pathway analyses of DGE genes indicating the top 10 up-regulated
851 pathways in explants cultures in **(A)** 1% oxygen and **(B)** 20% oxygen. Adjusted *p* values (Bonferroni)
852 and the number of genes identified in each pathway category is represented beside each plot. **(C)**
853 Dendrogram depicts hierarchical clustering of 1%, 5%, and 20% oxygen cultured column trophoblasts
854 using a proliferation-specific GO signature (Nuclear Division; 93 genes). Within the heatmap, brown =
855 low expression; white = mid-level expression; green = high expression. For each sample, oxygen
856 condition (1% = blue 5% = purple; 20% = red) is indicated, as is the unique placental sample/patient ID
857 used to generate the explant (indicated by shade of grey). **(D)** Representative immunofluorescence
858 images of BrdU signal (green) within placental explant columns cultured in 1%, 5%, or 20% oxygen.
859 Trophoblasts are identified by KRT7 signal (magenta). Bar = 100 μm. **(E)** Bar/scatter plots show
860 quantification of BrdU incorporation into column trophoblasts cultured in 1%, 5%, or 20% oxygen.
861 Median values are shown and statistical analyses between groups were performed using ANOVA and
862 two-tailed Tukey post-test; significance $p < 0.05$.
863

Figure 5. Low oxygen drives column cell differentiation along the EVT pathway. **(A)** Previously published scRNAseq data (Vento-Tormo et al., 2018) for 14,366 trophoblast cells from first trimester placentae (n=5) were selected for investigating the cell-specificity of our list of identified oxygen-associated gene expression changes. Uniform Manifold Approximation and Projection (UMAP) (Becht et al., 2018) was used to visualize and cluster the cells after subsetting from other cell types in the published dataset. Cells are labelled according to their previous characterization (Vento-Tormo et al., 2018). **(B)** UMAP clusters cells by gene expression of canonical trophoblast marker genes. **(C)** Heatmap of top 15 genes upregulated in 1% and 20% oxygen. Also shown are genes aligning with general trophoblasts, villous cytotrophoblasts (CTB), proximal column trophoblast (PCT), and distal column trophoblast (DCT)/extravillous trophoblast (EVT). Geneset expression patterns are compared to averaged gene expression levels within single-cell informed cell types (CTB, proliferative CTB, EVT, proliferative EVT, SCT). **(D)** Pseudotime analysis was applied using Monocle 2 (Qiu et al., 2017; Trapnell et al., 2014) to visualize gene expression across trophoblast differentiation. Two lineage trajectories were identified corresponding to the extravillous pathway and villous pathway. A cell state of origin is also shown. **(E)** The inferred trajectory resulted into two distinct endpoints: one branch leading to cells highly expressing SCT markers (e.g. ERVFRD-1), and another leading to cells highly expressing EVT markers (HLA-G). **(F)** A heatmap was constructed using inferred pseudotime and the top 15 upregulated genes in 1% and in 20% oxygen conditions. Pseudotime was ordered such that the left and right ends represent the EVT and SCT endpoints. Hierarchical clustering was applied to the genes (ordered along the rows) and separated into 5 clusters.

885 **Figure 6.** Low oxygen exposure promotes column-specific expression of *LOX*. **(A)** Gene array box-
886 plot expression levels of *LOX* mRNA in placental explants cultured in 1%, 5%, and 20% oxygen. **(B)**
887 Representative image showing *LOX* mRNA transcript *in situ* localization (dark pink signal) within a
888 first trimester placental villus. The hashed box outlines the enlarged region to the right. Shown are
889 annotations of trophoblast/placental subtypes; Mesenchymal core (MC), cytotrophoblast (CTB),
890 syncytiotrophoblast (SCT), proximal column trophoblast (PCT), distal column trophoblast (DCT).
891 Shown as an inset is an immunofluorescent image depicting nuclei (DAPI; blue), keratin-7 (K7;
892 magenta), and HLA-G (orange) localization within a serial section of the same placental villus. Bars =
893 100 μm. **(C)** Representative images of *LOX* mRNA localization within placental explants cultured in
894 1% or 20% oxygen. Specific trophoblast subtypes are indicated as above, and the hashed box
895 corresponds to the enlarged area shown below. Also shown are insets of immunofluorescent images
896 depicting nuclei (DAPI; blue), keratin-7 (K7; magenta), and HLA-G (orange) localization within
897 corresponding serial sectioned regions of the explant. Bars = 100 μm. **(D)** Bar/scatter plots show LOX
898 activity levels within conditioned media (CM) of placental explants cultured in either 1% or 20%
899 oxygen in the presence/absence of the LOX inhibitor BAPN (5 mM). Recombinant active lysyl oxidase
900 (rLOX) served as a positive control whereas explant culture media alone served as a negative control.
901 Activity corresponds to level of fluorescence intensity (590 nm). Median values are shown and
902 statistical analyses between groups were performed using ANOVA and two-tailed Tukey post-test;
903 significance $p < 0.05$.
904
905

906 **Figure 7.** Inhibition of lysyl oxidase (LOX) dampens column outgrowth. **(A)** Bar/scatter plots show
907 LOX activity levels within conditioned media (CM) of placental explants cultured in 1% oxygen in the
908 presence/absence of BAPN (500 μM). Recombinant active lysyl oxidase (rLOX) served as a positive
909 with explant culture media alone served as a negative control. Activity corresponds to level of
910 fluorescence intensity (590 nm). Median values are shown and statistical analyses between groups were
911 performed using ANOVA and two-tailed Tukey post-test. **(B)** Representative images of villous
912 explants (n=3 distinct placentae; multiple explants per placenta) cultured in 1% oxygen and in the
913 presence/absence of BAPN (500 μM). Column outgrowth is shown at 0hr and 48 hr of culture. **(C)** Box
914 plots showing the fold-change of column outgrowth between 48 hr and 0 hr following treatment with
915 BAPN. Median values are shown and statistical analyses between groups were performed using
916 ANOVA and two-tailed Tukey post-test; significance $p < 0.05$.
917
918

919 **Supplemental Figure Legends**

920 **Supplemental Figure 1.** Normalization and PCA analysis of placental explant gene microarray data.
921 Average expression values for each explant sample **(A)** before and **(B)** after quantile normalization and
922 filtering/removal of probes. **(C and D)** Principal component analysis (PCA) of raw data, normalized
923 data, and filtered data.

924

925 **Supplemental Figure 2.** Pathway analyses of unique gene signatures of 1% and 5% oxygen-cultured
926 explants. **(A)** Top 20 gene pathways upregulated exclusively in 1% oxygen when compared to 20%
927 oxygen. **(B)** Top 20 gene pathways exclusively upregulated in 5% oxygen when compared to 20%
928 oxygen. The size of the dot represents the number of significant genes in the pathway and the colour
929 represents adjusted *P*-values as indicated in the legend.

930

931 **Supplemental Figure 3.** Top gene pathways identified in explant columns cultured in 5% oxygen. Top
932 20 pathways upregulated in 5% oxygen when compared to 20% oxygen. The size of the dot represents
933 the number of significant genes in the pathway and the colour represents adjusted *P*-values as indicated
934 in the legend.

935

936 **Supplemental Figure 4.** Low oxygen culture promotes trophoblastic and EVT gene signatures in
937 placental explants. **(A)** Dendrogram depicts hierarchical clustering of 1%, 5%, and 20% oxygen
938 cultured column trophoblasts using the respective 14-gene signature. The heatmap displays expression
939 profiles of trophoblast genes identified as being significantly different between 1%, 5%, and 20%
940 cultures. Within the heatmap, brown = low expression; white = mid-level expression; green = high
941 expression. For each sample, oxygen condition (1% = blue 5% = purple; 20% = red) is indicated, as is
942 the unique placental sample/patient ID used to generate the explant (indicated by shade of grey).

943 Representative immunofluorescence images showing expression of PEG10 (magenta) within **(B)** first
944 trimester placental villi and **(C)** Matrigel-imbedded placental explants cultured in either 1%, 5%, or
945 20% oxygen. Trophoblast are identified by keratin-7 staining (KRT7; green) and nuclei are stained
946 with DAPI (white). Shown are specific cell types: Syncytiotrophoblast (SCT), villous cytotrophoblasts
947 (CTB), proximal column trophoblast (PCT), distal column trophoblast (DCT), and the mesenchymal
948 core (MC). Bar = 100 μm**.**
949

Figure 1

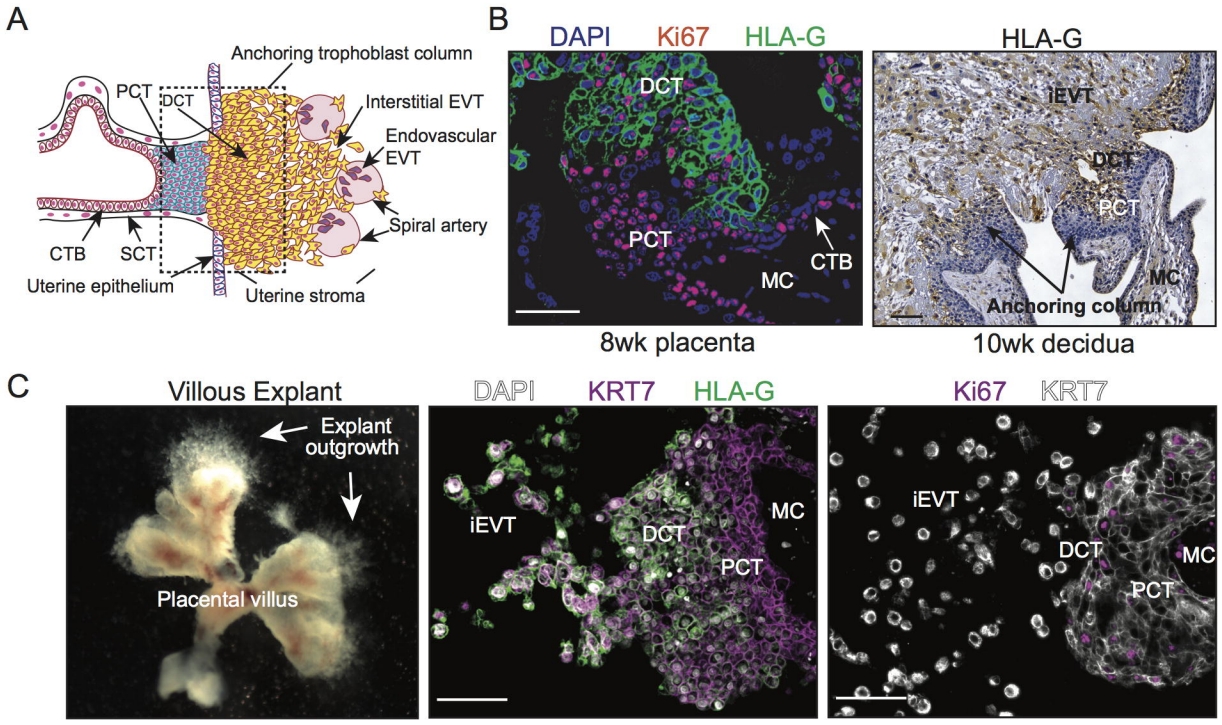
A
Anchoring trophoblast column
PCT
DCT
Interstitial EVT
Endovascular EVT
Spiral artery
CTB
SCT
Uterine epithelium
Uterine stroma
B
DAPI
Ki67
HLA-G
DCT
PCT
CTB
MC
8wk placenta
HLA-G
iEVT
DCT
PCT
MC
Anchoring column
10wk decidua
C
Villous Explant
Explant outgrowth
Placental villus
DAPI
KRT7
HLA-G
iEVT
DCT
MC
PCT
Ki67
KRT7
iEVT
DCT
MC
PCT

Figure 2

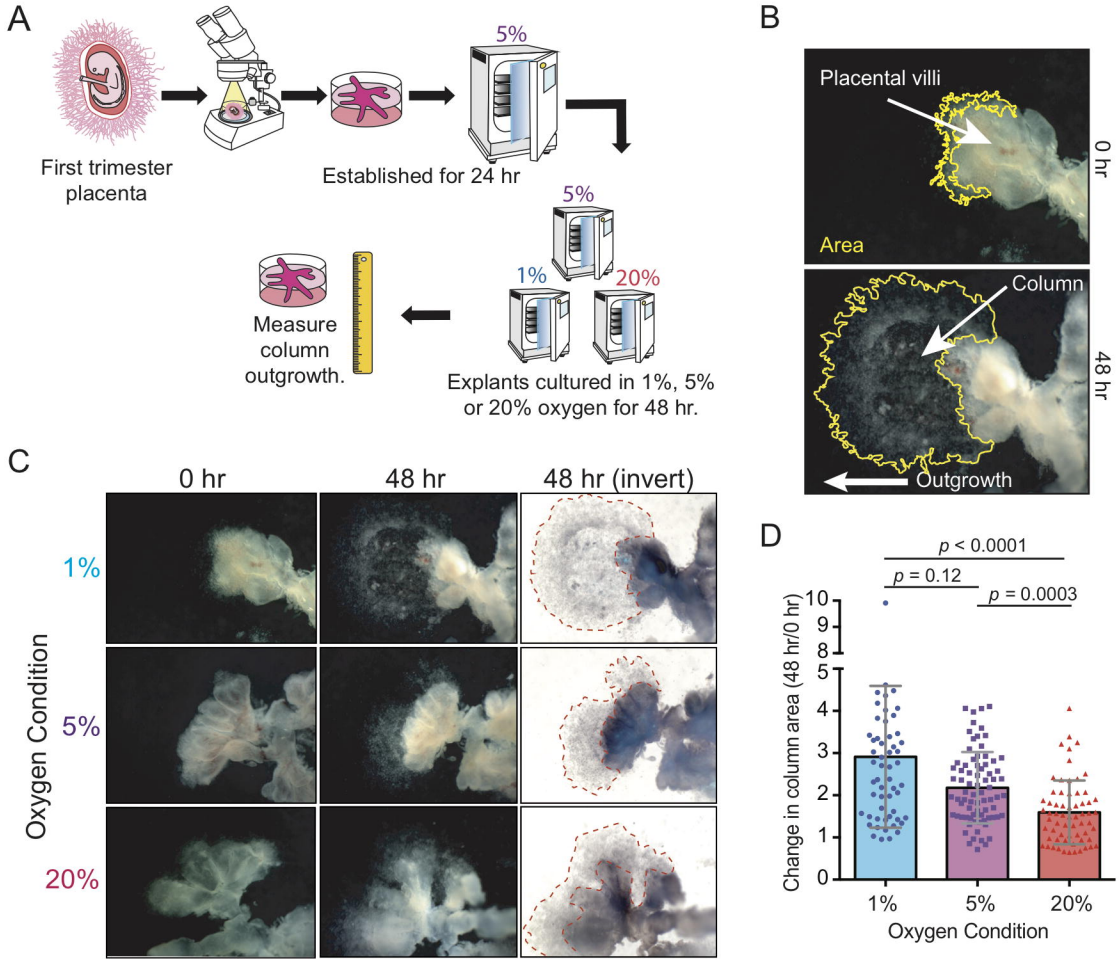
A
First trimester placenta
Established for 24 hr
5%
1%
20%
Explants cultured in 1%, 5% or 20% oxygen for 48 hr.
Measure column outgrowth.
B
Placental villi
Area
0 hr
Column
Outgrowth
48 hr
C
0 hr
48 hr
48 hr (invert)
Oxygen Condition
1%
5%
20%
D
p < 0.0001
p = 0.12
p = 0.0003
Change in column area (48 hr/0 hr)
Oxygen Condition

Figure 3

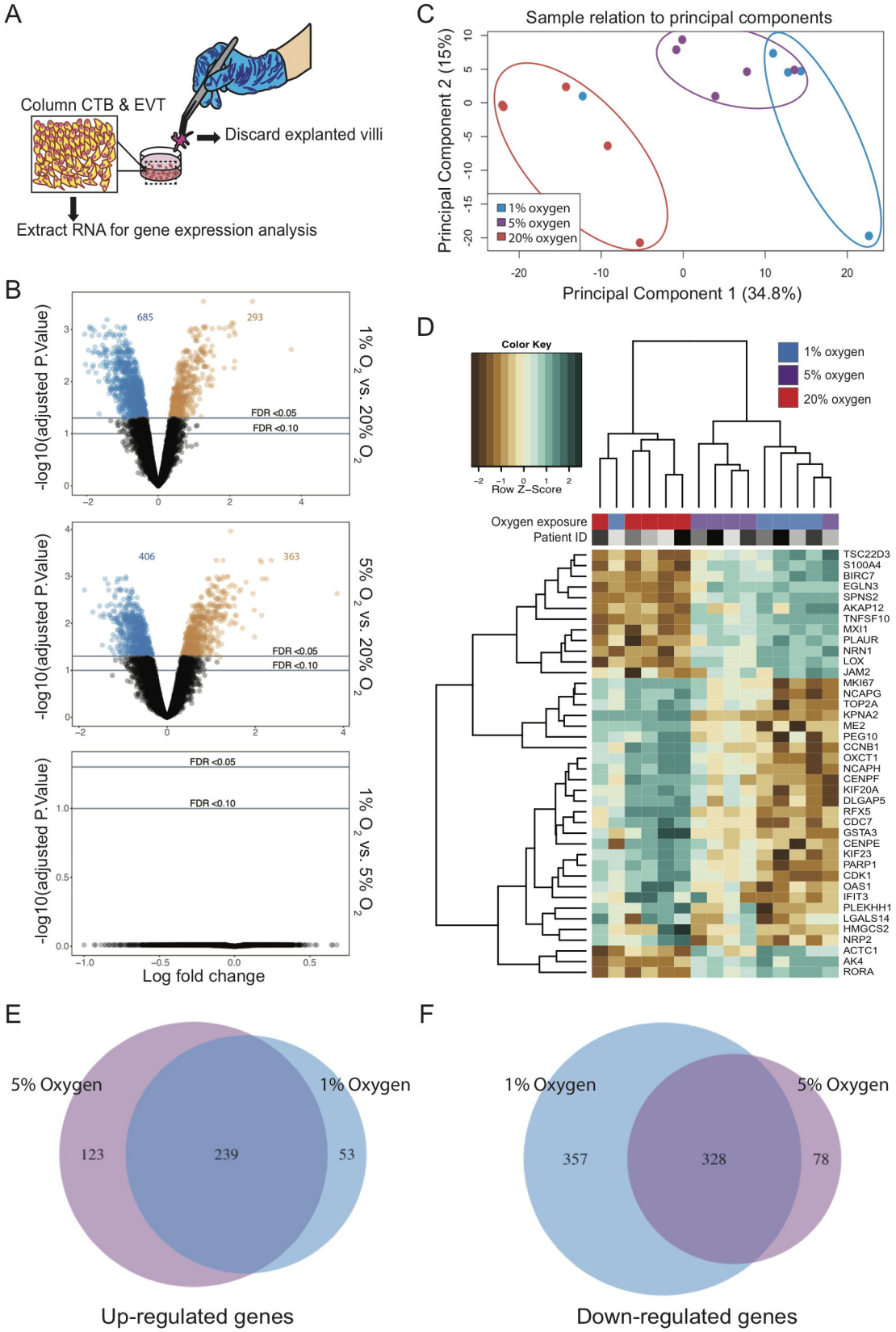
A
Column CTB & EVT
Discard explanted villi
Extract RNA for gene expression analysis
B
685
293
FDR <0.05
FDR <0.10
1% O2 vs. 20% O2
406
363
5% O2 vs. 20% O2
1% O2 vs. 5% O2
-log10(adjusted P.Value)
Log fold change
C
Sample relation to principal components
Principal Component 2 (15%)
Principal Component 1 (34.8%)
1% oxygen
5% oxygen
20% oxygen
D
Color Key
Row Z-Score
Oxygen exposure
Patient ID
TSC22D3
S100A4
BIRC7
EGLN3
SPNS2
AKAP12
TNFSF10
MXI1
PLAUR
NRN1
LOX
JAM2
MKI67
NCAPG
TOP2A
KPNA2
ME2
PEG10
CCNB1
OXCT1
NCAPH
CENPF
KIF20A
DLGAP5
RFX5
CDC7
GSTA3
CENPE
KIF23
PARP1
CDK1
OAS1
IFIT3
PLEKHH1
LGALS14
HMGCS2
NRP2
ACTC1
AK4
RORA
E
5% Oxygen
1% Oxygen
123
239
53
Up-regulated genes
F
1% Oxygen
5% Oxygen
357
328
78
Down-regulated genes

Figure 4

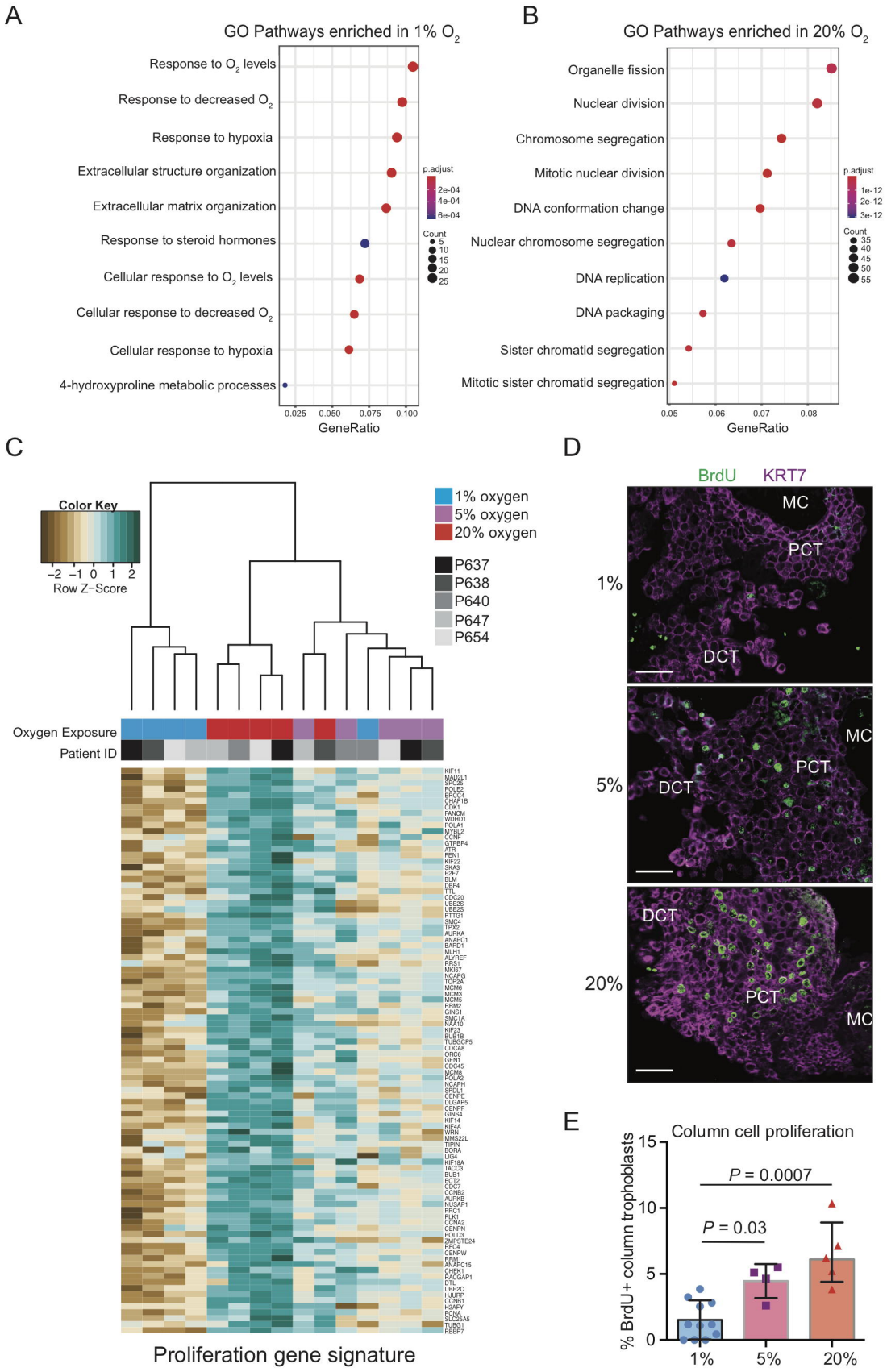
A
GO Pathways enriched in 1% O_2
Response to O_2 levels
Response to decreased O_2
Response to hypoxia
Extracellular structure organization
Extracellular matrix organization
Response to steroid hormones
Cellular response to O_2 levels
Cellular response to decreased O_2
Cellular response to hypoxia
4-hydroxyproline metabolic processes
p.adjust
2e-04
4e-04
6e-04
Count
5
10
15
20
25
0.025
0.050
0.075
0.100
GeneRatio
B
GO Pathways enriched in 20% O_2
Organelle fission
Nuclear division
Chromosome segregation
Mitotic nuclear division
DNA conformation change
Nuclear chromosome segregation
DNA replication
DNA packaging
Sister chromatid segregation
Mitotic sister chromatid segregation
p.adjust
1e-12
2e-12
3e-12
Count
35
40
45
50
55
0.05
0.06
0.07
0.08
GeneRatio
C
Color Key
−2 −1 0 1 2
Row Z−Score
1% oxygen
5% oxygen
20% oxygen
P637
P638
P640
P647
P654
Oxygen Exposure
Patient ID
Proliferation gene signature
D
BrdU
KRT7
1%
5%
20%
MC
PCT
DCT
E
Column cell proliferation
% BrdU+ column trophoblasts
P = 0.0007
P = 0.03
0
5
10
15
1%
5%
20%

Figure 5

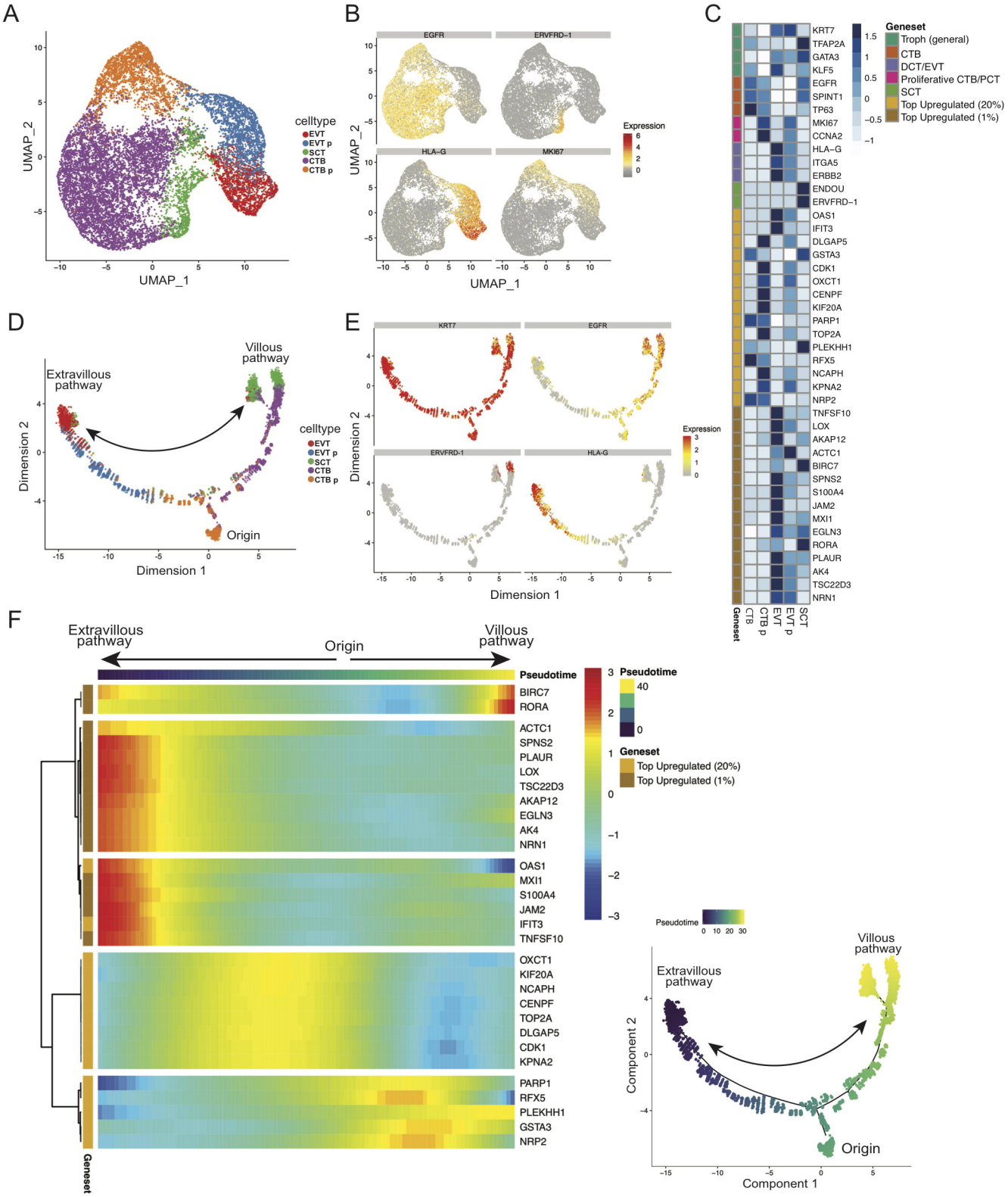
A
UMAP_2
UMAP_1
celltype
EVT
EVT p
SCT
CTB
CTB p
B
EGFR
ERVFRD−1
HLA−G
MKI67
Expression
C
Geneset
Troph (general)
CTB
DCT/EVT
Proliferative CTB/PCT
SCT
Top Upregulated (20%)
Top Upregulated (1%)
KRT7
TFAP2A
GATA3
KLF5
EGFR
SPINT1
TP63
MKI67
CCNA2
HLA−G
ITGA5
ERBB2
ENDOU
ERVFRD−1
OAS1
IFIT3
DLGAP5
GSTA3
CDK1
OXCT1
CENPF
KIF20A
PARP1
TOP2A
PLEKHH1
RFX5
NCAPH
KPNA2
NRP2
TNFSF10
LOX
AKAP12
ACTC1
BIRC7
SPNS2
S100A4
JAM2
MXI1
EGLN3
RORA
PLAUR
AK4
TSC22D3
NRN1
CTB
CTB p
EVT
EVT p
SCT
D
Extravillous pathway
Villous pathway
Origin
Dimension 2
Dimension 1
E
KRT7
EGFR
ERVFRD-1
HLA-G
F
Extravillous pathway
Origin
Villous pathway
Pseudotime
Geneset
Top Upregulated (20%)
Top Upregulated (1%)
BIRC7
RORA
ACTC1
SPNS2
PLAUR
LOX
TSC22D3
AKAP12
EGLN3
AK4
NRN1
OAS1
MXI1
S100A4
JAM2
IFIT3
TNFSF10
OXCT1
KIF20A
NCAPH
CENPF
TOP2A
DLGAP5
CDK1
KPNA2
PARP1
RFX5
PLEKHH1
GSTA3
NRP2
Component 2
Component 1

Figure 6

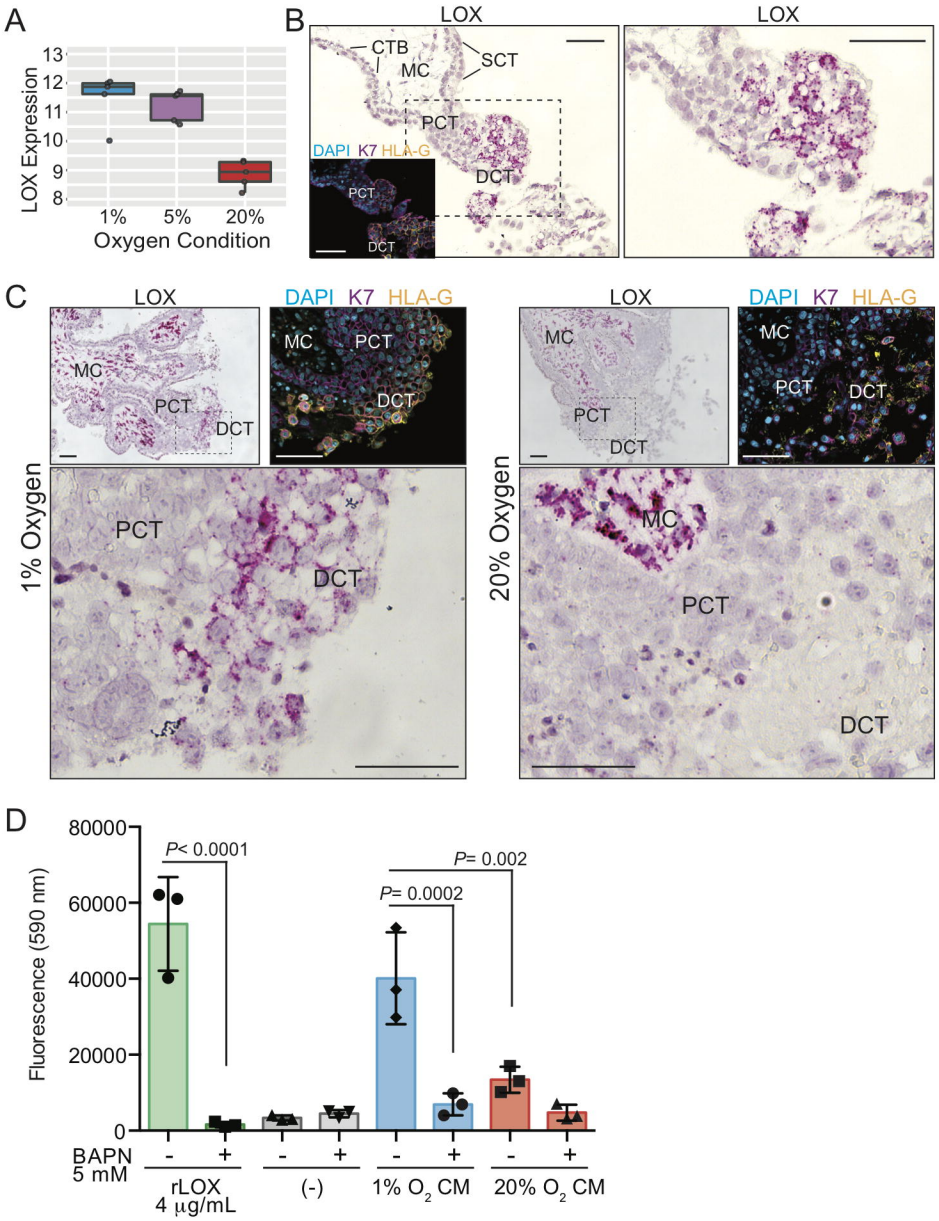
A
LOX Expression
13
12
11
10
9
8
1%
5%
20%
Oxygen Condition
B
LOX
CTB
MC
SCT
PCT
DCT
DAPI K7 HLA-G
PCT
DCT
LOX
C
LOX
DAPI K7 HLA-G
MC
PCT
DCT
1% Oxygen
PCT
DCT
LOX
DAPI K7 HLA-G
MC
PCT
DCT
20% Oxygen
MC
PCT
DCT
D
Fluorescence (590 nm)
80000
60000
40000
20000
0
P< 0.0001
P= 0.0002
P= 0.002
BAPN 5 mM
-
+
rLOX 4 μg/mL
(-)
1% O2 CM
20% O2 CM

Figure 7

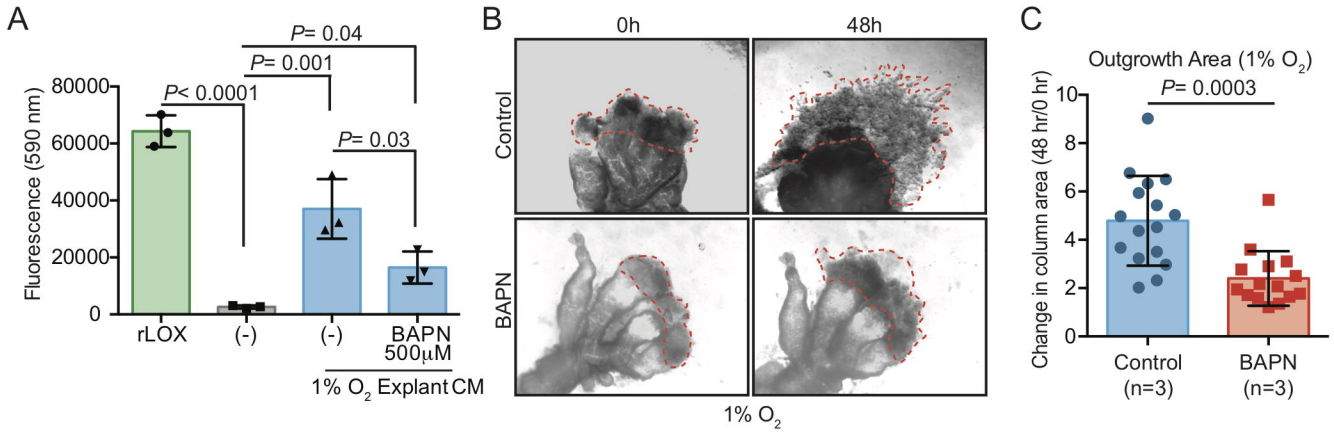
A
P= 0.04
P= 0.001
P< 0.0001
P= 0.03
Fluorescence (590 nm)
80000
60000
40000
20000
0
rLOX
(-)
(-)
BAPN
500μM
1% O2 Explant CM
B
0h
48h
Control
BAPN
1% O2
C
Outgrowth Area (1% O2)
P= 0.0003
Change in column area (48 hr/0 hr)
10
8
6
4
2
0
Control
(n=3)
BAPN
(n=3)